NASA TECHNICAL NOTE

DESCRIPTION OF THE HIGH-ENTHALPY ARC TUNNEL AT THE LANGLEY RESEARCH CENTER INCLUDING TEST-STREAM CONDITIONS AT SELECTED OPERATING POINTS

by William L. Wells

Langley Research Center
Langley Station, Hampton, Va.

DESCRIPTION OF THE HIGH-ENTHALPY ARC TUNNEL AT

THE LANGLEY RESEARCH CENTER INCLUDING

TEST-STREAM CONDITIONS AT SELECTED

OPERATING POINTS

By William L. Wells

Langley Research Center
Langley Station, Hampton, Va.

NATIONAL AERONAUTICS AND SPACE ADMINISTRATION

DESCRIPTION OF THE HIGH-ENTHALPY ARC TUNNEL AT

THE LANGLEY RESEARCH CENTER INCLUDING

TEST-STREAM CONDITIONS AT SELECTED

OPERATING POINTS

By William L. Wells
Langley Research Center

SUMMARY

The high-enthalpy arc tunnel at the Langley Research Center consists of a 4-megawatt direct-current power supply, a 75 000-foot^3 (2120-meter^3) pump-down vacuum system, a commercial long-axial-arc gas heater, a free-jet test section, and necessary high-pressure cooling-water and test-gas systems. Three supersonic conical nozzle lengths are used to provide a wide range of test-stream parameters. The nozzle-exit radii are 1.00 inch (2.54 cm), 2.30 inches (5.84 cm), and 3.82 inches (9.70 cm).

The arc gas heater was operated at chamber pressures from 1.2 to 3.3 atm (1 atm = 1.013×10^5 N/m^2) with corresponding air mass-flow rates from about 0.02 to 0.08 lb/sec (9.07 to 36.3 g/sec). Stagnation pressures behind the normal shock measured at the stream center line cover a range from about 0.03 to 0.72 atm and cold-wall heating rates range from about 200 to 903 Btu/ft^2-sec (227 to 1025 W/cm^2) on a 1-inch-diameter (2.54-cm) flat-faced probe. Calculated enthalpies based on these measurements range from about 10 000 to 13 000 Btu/lb (23.2 to 30.2 MJ/kg).

In the two largest nozzles, measurements of heating rate and pressure across the test stream at three different distances from each nozzle exit indicate reasonably flat profiles across at least 60 percent of the stream.

In all three nozzles, measurements were made of pressure and heating-rate distributions on a specific probe shape. Graphical comparisons show reasonably good agreement between the measured heating-rate distributions and theory and between the measured pressure distributions and data from a tunnel where the flow is known to be smooth and uniform.

INTRODUCTION

A continuing effort is made at Langley Research Center to improve and expand the test conditions available in ground-based facilities for the simulation of aerodynamic

forces and heating encountered during the entry of spacecraft into the earth's atmosphere. Because the conditions of atmospheric entry vary so greatly with altitude and spacecraft velocity, a number of facilities are needed for simulation of the full range of these conditions. As a part of the effort to expand this simulation range, the high-enthalpy arc tunnel at the Langley Research Center was put into operation. The utility of a given tunnel of this type can be increased by the use of several nozzles so that the amount of test-stream expansion can be varied. In this high-enthalpy arc tunnel, the conical nozzle is made in sections so that three nozzle-exit diameters are available.

This paper briefly describes the tunnel and also presents the results of measurements made to determine the size and uniformity of the test stream for three arc-heater operating conditions with air as the test gas. The measurements include surveys across the stream of stagnation-point pressure and heating rate on a probe and also the pressure and heating-rate distribution on a specific probe shape located at the nozzle center line. Measurements were made at various distances from each nozzle exit. Test-stream parameters are also presented which were calculated assuming nonequilibrium flow in the nozzles.

SYMBOLS

The units used for the physical quantities defined in this paper are given both in the U.S. Customary Units and in the International System of Units (SI). Factors relating the two systems are given in reference 1.

A	cross-sectional area of nozzle
c	specific heat
H	enthalpy
M	Mach number
N_{Re}	Reynolds number
p	pressure
$\dot{q}$	heating rate
r	radial distance from test-stream center line to probe location

R	radius
S	distance from probe center line along probe surface
t	time
T	temperature
V	velocity
x	linear distance from the nozzle-exit plane along the test-stream axis
μ	viscosity
ρ	density
τ	effective wall thickness of heat-transfer probe (ratio of volume to unit surface area)

Subscripts:

B	probe body
c	corner
CL	center line
E	nozzle exit
min	nozzle minimum
n	probe nose
t	total or stagnation
w	conditions at the probe wall
1	in the arc chamber

2   behind the normal shock

∞   free stream

TUNNEL DESCRIPTION

A sketch of the tunnel is shown in figure 1.   Basically, the tunnel consists of a dc arc heater, conical nozzle, free-jet test section, straight-pipe diffuser, aftercooler, test-section-pressure control valve, and 75 000 feet^3 (2120 meters^3) of vacuum-sphere space. The test air is regulated from a compressed-air storage supply, and cooling water for the arc heater and aftercooler is supplied by a 300-psi (207-N/cm^2) pump from a cooled reservoir.

Arc Heater and Power Supply

A cross-sectional view of the dc arc heater is shown in figure 2.   It is a long-axial-arc heater which is similar to that described in reference 2.   The rear electrode (anode) and front electrode (cathode) are tube shaped, made of copper, and water cooled.   A small magnet coil is mounted over the rear electrode to rotate the arc attachment point within that electrode and thus avoid immediate burnout.   The air or test gas is introduced tangentially into the center chamber through eight small (0.040-inch-diameter (0.102-cm)) orifices thereby creating vortex flow which rotates and stabilizes the arc within the front electrode.   The front electrode includes the nozzle entrance, the 0.75-inch-diameter (1.91-cm) throat and part of the expansion section.   A boron-nitride heat shield protects and insulates the part of the rear electrode which protrudes into the center chamber. Two pressure-measurement orifices are located in the heater walls, one in the center chamber and one in the rear end of the rear electrode.

The dc power supply consists of lead-acid batteries connected to provide 1500 volts at open circuit and currents up to 3000 amperes.   (During a run, the current decreases at the rate of about 3 percent per minute.)   For a given tunnel operating condition, the current is regulated by water-cooled stainless-steel tube resistors added to the circuit.   The magnet coil operates from a similar, but separate, power supply which has an open-circuit voltage of 125 volts.   A schematic diagram of the power circuits is presented in figure 3.

Test Section

The test section, which is a steel box with dimensions of 24 × 24 × 38 inches (61.0 × 61.0 × 96.5 cm) and with three observation windows, encloses the nozzle-expansion sections, two model-insertion mechanisms, and a movable diffuser inlet.

4

(See figs. 1 and 4.) The 8° (0.14-radian) half-angle conical nozzle is made in three sections which provide exit radii of 3.82 inches (9.7 cm), 2.30 inches (5.84 cm), and 1.00 inch (2.54 cm). (See figs. 5(a), 5(b), and 5(c).) The model-insertion mechanisms are the swing-in type and are operated by pneumatic cylinders. Both inserters can be manually moved along the axis of the test section to provide the proper location of the test model with respect to the desired nozzle exit.

Test-Section-Pressure Control Valve

The aftercooler is connected to the vacuum system through a 16-inch-diameter (40.6-cm) pipe. A remotely operated butterfly valve is located in this pipe to restrict the flow when higher test-section pressures are needed to match the free-stream exit pressures in the smaller nozzles.

INSTRUMENTATION

Currents and voltages were measured by using shunts and voltage dividers, respectively, which were located in the circuits as shown in figure 3. All pressures were measured with strain-gage transducers, and all temperatures were measured with thermocouples. Air mass-flow rates were measured with a sharp-edge-orifice meter. When a probe was to be inserted slowly for heating-rate-distribution measurements across the stream, a Wheatstone bridge with a slide-wire resistor was used to determine the location of the probe within the stream at any time. The slide wire was connected to the inserter and the circuit was calibrated before use. All of the above measurements were recorded continuously on an oscillograph recorder. For the thermocouples on the transient heat-transfer probes, the oscillograph galvanometer elements had a response time of 0.926 msec.

Steady-State Heat-Transfer Probe

The steady-state heat-transfer probe is a commercially made 1-inch-diameter (2.54-cm) flat-faced calorimeter. Since this calorimeter is water cooled, it can be kept in the test stream as long as desirable. A photograph of this probe is shown in figure 6(a). When heat is applied, the calorimeter has a continuous millivolt output due to its construction which, basically, is a thermocouple consisting of a constantan-foil disk which is soldered at its perimeter to a water-cooled copper block. A copper lead wire is attached to the center of the foil disk and another one is attached to the copper block. A heat flux on the face of the calorimeter generates a heat flow radially from the center of the constantan disk to the cooled copper block and generates a millivolt output. The millivolt output is measured in the circuit formed by the copper wire, the constantan foil,

and the copper block. The hot junction is the wire-to-foil connection and the cold junction is the foil-to-copper-block connection. The millivolt output is an indication of the heating rate. The probe was calibrated with a radiant heat source before use. The information necessary to determine the sensitivity and time constant for this type of calorimeter is given in reference 3.

Transient Heat-Transfer Probe

The transient heat-transfer probe is a 1-inch-diameter (2.54-cm) flat-faced stainless-steel cylinder. A thermocouple is located on the back surface of the flat face at the probe center line. The measured wall thickness at the thermocouple is 0.075 inch (0.191 cm). (See fig. 6(b).)

Pressure Rake

The uncooled pressure rake provided a method of inserting several pressure probes into the test stream simultaneously for measurement of pressure distribution across the stream. The rake consists of a flat steel bar with copper tubes of 0.120-inch (0.305-cm) inside diameter silver soldered into drilled holes as shown in figure 6(c). The tubes, or probes, were located 0.5 inch (1.27 cm) apart and protruded more than 0.375 inch (0.953 cm) from the steel surface.

Transient Heat-Transfer-Distribution Probe

The heat-transfer-distribution probe is a 1.5-inch-diameter (3.81-cm) thin-wall inconel cylinder with a ratio of nose to body radius of 3.14 and a ratio of corner to body radius of 0.28. Thermocouples are located along the back surface of the probe as shown in figure 7. The wall thickness was measured at each thermocouple location. (Nominal wall thickness is 0.050 inch (0.127 cm).)

Pressure-Distribution Probe

The pressure-distribution probe is a 1.5-inch-diameter (3.81-cm) water-cooled copper cylinder with a ratio of nose to body radius of 3.14 and a ratio of corner to body radius of 0.28. Pressure orifices are located along the surface of the probe as shown in figure 8. (In the smallest nozzle a 1.0-inch-diameter (2.54-cm) probe with the same radius ratios was used.)

TEST PROCEDURES

Measurements in the Test Stream

Measurements of arc current, cooling-water temperature rise, and so on, indicated that the system had reached equilibrium operating conditions by 30 seconds of run time. All measurements in the test stream were made after equilibrium operating conditions had been reached. Measurements of heating rate and pressure were made across the stream and also on a certain probe shape. Survey measurements of heating rate and pressure across the stream were not made in the 1.00-inch-radius (2.54-cm) nozzle because the diameter of the steady-state heat-transfer probe was the same as the nozzle radius. Measurements were made at various distances from each nozzle exit for each arc-heater operating condition investigated. These distances were a function of nozzle-exit radius R_E and, in general, were $0.4R_E$, $0.8R_E$, and $1.2R_E$.

Measurements of pitot pressure across the stream were made with a rake which was inserted into the stream and left long enough for each measurement to reach an equilibrium value as indicated by oscillograph traces. Stagnation-point heating rates across the stream were measured with the steady-state heat-transfer probe which was slowly inserted into the stream at a rate of about 0.29 in./sec (0.74 cm/sec) until it arrived at the geometric center line of the nozzle. The probe was then left at the center line for about 5 seconds before being retracted.

Measurements of heating rate and pressure distribution on a specific model design were made by quickly inserting each model to the geometric center line of the nozzle.

The measurements were made with the tunnel operating at three different arc-heater conditions which were felt to be representative of the achievable conditions with this system.

Heating-Rate and Enthalpy Determination

Heating-rate determination with the steady-state heat-transfer probe was accomplished with the measured millivolt output and the earlier probe calibration. Heat-transfer rates were calculated on the transient heat-transfer probes at the thermocouple locations by using the rate of measured temperature rise of the back surface of the material. The heat-transfer-rate equation used was

$$\dot{q} = \rho c \tau \frac{dT}{dt}$$

The dT/dt part of the equation was obtained by recording temperature with respect to time and the remaining quantities are a function of material and location on the probe surface. The slope of the temperature trace was obtained after it became linear with time, usually after the wall temperature had reached about 300° F (149° C).

The stream enthalpy along the nozzle center line was calculated by using measured values of pressure and heating rate and the heat-transfer theory of Fay and Riddell (ref. 4).

RESULTS AND DISCUSSION

In general, the overall system worked very well and good repeatability of arc-heater and test-stream conditions was obtained. A survey was made of the range of operation of the electric arc heater with air and the reported power supply and circuit arrangement. Representative conditions at which the arc-heater characteristics and test stream appeared most stable were selected for further exploration as reported herein. A more exhaustive study would undoubtedly show that the tunnel could be successfully operated at other heater conditions which do not deviate greatly from those reported in this paper.

Arc Heater

For the same preset conditions the arc heater will repeat power input from run to run within about 3 percent. Table I summarizes the arc-heater conditions that were used for the tests reported herein. The arc-chamber pressure shown was measured at the back of the rear electrode. (See fig. 2.) In reference 2, good agreement was reported for pressures measured at this point and those at a settling chamber just upstream of the nozzle entrance. The efficiency shown in table I is the ratio of the energy input to the test gas, as determined by an energy balance, to the power input to the arc. An indication of arc-heater stability is indicated by strip-chart-recorder traces of arc current and voltage for a typical run as shown in figure 9.

Because of the initial weight of the electrodes and the relatively large amounts of electrode material loss at failure, accurate measurements of stream contamination have not been obtained. A rough estimate of stream contamination, however, is about 0.15 percent by weight.

Erosion was more severe in the front electrode (cathode) than in the rear electrode (anode). Furthermore, the erosion in the front electrode occurred in a spiral pattern and in a ring pattern in the rear electrode. An interesting point is that imminent failure of the electrode due to erosion is not readily apparent by observation or measurement of its inside diameter when the heater is operated in the range of pressures reported here.

Apparently, as the copper wall becomes thinner, the high-pressure cooling water pushes the wall inward to maintain a nearly constant inside diameter. Figure 10 shows part of a front electrode that was sectioned before failure but after about 1.4 hours of intermittent operation. Another front electrode that was run until failure lasted for about 3.5 hours of intermittent operation. Figure 11 shows a sectioned part of a rear electrode that failed after about 3.9 hours of intermittent operation. These electrodes were used under the conditions shown in table I.

One other source of trouble, although relatively insignificant, was the boron-nitride heat shield. After a few runs, one side of the heat-shield ring cracked, possibly because of expansion. However, the heat shield was continued in use for many runs before the other side of the ring broke and replacement was necessary. (See fig. 12.)

Test-Stream Measurements

Test-stream surveys.- In the two largest nozzles, surveys of stagnation pressure behind the normal shock $p_{t,2}$ and stagnation cold-wall heating rate $\dot{q}$ across the test stream were made. These measurements were made from the center line radially outward to the edge of the stream. (This measurement was not made in the smallest nozzle because the probe sizes were large relative to the nozzle radius.) These measurements were made for each of the three arc-heater conditions listed in table I. Furthermore, for each condition the surveys were made at three different distances x from each nozzle-exit plane. The results of these measurements are shown in figures 13(a), 13(b), and 13(c) for the 3.82-inch-radius (9.7-cm) nozzle and in figures 14(a), 14(b), and 14(c) for the 2.30-inch-radius (5.84-cm) nozzle. In these figures the probe location with respect to the stream center line is presented on the abscissa as a ratio of the radial distance from the center line r to the nozzle-exit radius R_E.

Both the $p_{t,2}$ and $\dot{q}$ curves have a plateau, or a reasonably constant part, that extends across at least 60 percent of the radius for all conditions and distances x for the 3.82-inch-radius (9.7-cm) nozzle. For the 2.30-inch-radius (5.84-cm) nozzle, the plateau extends across about 60 percent or more of the exit radius although it is not quite as constant as it is for the larger nozzle. For either nozzle a decrease in $p_{t,2}$ is evident for a given tunnel condition as the distance from the nozzle x is increased; thus, some continuation in stream expansion after leaving the conical nozzle is indicated.

Probe distributions.- The distributions of pressure and heating rate on a specific probe design were measured in each nozzle and for each of the arc-heater conditions listed in table I. These measurements were made with the probe located at the stream center line and at a distance from the nozzle exit x of $0.8R_E$. The probes used for

these measurements are shown in figures 7 and 8. (The probes used in the 1.00-inch-radius (2.54-cm) nozzle were of the same design but had a 1-inch (2.54-cm) diameter instead of a 1.5-inch (3.81-cm) diameter.)

The results of the pressure measurements were compared with data that were obtained in a wind tunnel where the flow is known to be smooth and uniform (See ref. 5.) The results of the heating-rate measurements were compared with theory derived from reference 6. These comparisons are presented for all three nozzles and all three arc-heater conditions in figures 15, 16, and 17. Figures 15(a) to 15(c) are for the 3.82-inch-radius (9.7-cm) nozzle, figures 16(a) to 16(c) are for the 2.30-inch-radius (5.84-cm) nozzle and figures 17(a) to 17(c) are for the 1.00-inch-radius (2.54-cm) nozzle. In these figures the ordinate presents the pressure and heating-rate measurement made at a given point on the probe surface compared with that made at the probe center line. The abscissa presents the location of the point at which the measurement was made as a function of the distance along the probe surface from the probe center line divided by the probe body radius.

In general, the measurements compare very favorably with the theory of reference 6 and the wind-tunnel data from reference 5. One exception noted throughout the heating-rate comparisons was that the theory indicated a peak heating rate at the point where the probe nose radius and corner radius met, but this peak was not indicated by the measurements. Heat conduction along the wall away from this point may account for some of this discrepancy. Also in the curves for the smallest nozzle (fig. 17) a distinct dip is noted, especially in the heating-rate data, at about one-half the probe radius. This may be related to some of the nonuniformity that can be seen in the stream survey measurements made in the larger nozzles. Overall, however, the test stream appears to be uniform and free from strong shocks.

Values of stagnation-point heating rate and pressure at the stream center line for the 1.00-inch-radius (2.54-cm) nozzle are shown in table II. (Comparable values for the other two nozzles were included in figs. 13 and 14.)

Stream enthalpy.- In figure 18 plots are shown of stream center-line heating rate and stagnation pressure behind the normal shock for all three nozzle stations; also shown are lines of constant enthalpy. The enthalpy was computed by using an approximate form of the Fay and Riddell equation (ref. 4) as follows:

$$k\left(H - H_w\right) = \dot{q}\left(\frac{R_{eff}}{p_{t,2}}\right)^{1/2}$$

where the constant k is 0.0392 and R_{eff} is the effective nose radius of the probe which was related to a hemispherical probe by the relation $0.54\dot{q}_{hemisphere} = \dot{q}_{flat\ face}$

(ref. 7). Different values of k can be found in the literature, reference 8, for instance, gives a value of k of 0.043 which was derived from the correlation of experimental data from several facilities with stream enthalpies from about 3000 to 35 000 Btu/lb (6.97 to 81.4 MJ/kg).

The points plotted on each figure indicate values of $\dot{q}$ and $p_{t,2}$ as measured at different distances x from each nozzle-exit plane. Figures 18(a), 18(b), and 18(c) are for the three arc-chamber pressures of 1.2 atm, 2.0 atm, and 3.3 atm, respectively. (Note: 1 atm = 1.013×10^5 N/m^2.) Corresponding arc-heater conditions can be found in table I. In any case a continual expansion of the stream after leaving the nozzle is indicated by the decreasing $\dot{q}$ and $p_{t,2}$ as the distance from the nozzle exit x is increased.

Overall, the indicated enthalpy range is from about 10 000 to about 13 000 Btu/lb (23.2 to 30.2 MJ/kg). Stagnation pressures behind the normal shock measured at the stream center line cover a range from about 0.03 to 0.72 atm and cold-wall heating rates range from about 200 to 903 Btu/ft^2-sec (227 to 1025 W/cm^2) on a 1-inch-diameter (2.54-cm) flat-faced probe.

The effect of gas dissociation on heating-rate measurements was not taken into account in these figures. That part of the stream energy which is required for dissociation is not available for heating and therefore the measured heating rate would indicate some value of enthalpy less than the true enthalpy if recombination did not occur behind the shock or at the probe surface. Most probe surface materials, especially metals, act as catalysts causing recombination of the dissociated gas to some degree. (See ref. 9.) In reference 8 this catalytic wall effect was investigated and it was concluded that for the range of conditions and the calorimeters used that the combined effects of nonequilibrium chemistry and surface catalysis were unimportant. In reference 10 it was indicated that for low-density, high-energy, nonequilibrium flows, errors in indicated enthalpy based on heating-rate measurements can be significant. Both of the above references included density and enthalpy values on the order of those reported in this paper. In reference 10 an equation is presented which can be used to predict the effects of recombination due to catalytic-wall effects. By using this relation for the worst condition presented in this paper, an upward correction in the presented enthalpy of about 17 percent is indicated. This worst condition occurs at the highest enthalpy and lowest free-stream density. In these calculations it was assumed that the flow through the shock layer was frozen and that the Lewis number and Schmidt number each had a value of unity. The value of the catalytic reaction-rate constant for the probe wall was assumed to be 173.2 in./sec (440 cm/sec). This value was taken from figure 6 of reference 9 for a nickel surface. This assumption seems valid since good agreement of heating rate was obtained for this condition when the thin-wall stainless-steel calorimeter shown in figure 6 of this paper

was used as compared with a nickel-plated-copper slug calorimeter as described in reference 11. Very little information is available concerning the catalytic reaction-rate constant for different materials and apparently the values vary for a specific material depending upon its cleanliness.

Another effect on heating rate, and thus on the indicated enthalpy, is that due to shock-generated vorticity at low Reynolds numbers. (See, for example, ref. 12.) For the same conditions just considered, a Reynolds number behind the shock of about 10^2 and a ratio of free-stream density to density behind the shock of about 0.17 were calculated. By using figure 5 of reference 12, a heating-rate, and thus an enthalpy, correction on the order of 13 percent is indicated. This correction is about the same as the correction due to noncatalytic-wall effects but in the opposite direction. Since these two corrections tend to cancel each other for these conditions, the uncorrected enthalpies indicated in figure 18 are believed to reflect a reasonable representation of the actual conditions.

When these types of calculations were made for the highest density and lowest enthalpy condition (highest arc-chamber pressure and smallest nozzle exit), no appreciable corrections were indicated for either the noncatalytic-wall effect or the low Reynolds number effect.

Calculated stream parameters and composition.- As an indication of free-stream conditions in each nozzle for the three reported heater operating conditions, table III presents calculated values of several stream parameters. The area ratios shown are for the geometrical throat and exit size. The stream constituents and all parameters except viscosity and Reynolds number were calculated with the computer program of reference 13 which considers nonequilibrium expansion of the gas in the nozzle.

Other constituents considered were molecular oxygen, nitric oxide, the positive ion of nitric oxide, and electrons; however, these species accounted for 0.1 percent of the flow or less and therefore were not included in the table. The values shown in the table were rounded off to three significant digits.

The viscosity for the mixture (based on the gas species shown in table III) was calculated by the method outlined in reference 14 and the individual specie viscosities required in this calculation were taken from reference 15.

CONCLUSIONS

The high-enthalpy arc tunnel at the Langley Research Center has been operated over an arc-heater pressure range from 1.2 to 3.3 atm (1 atm = 1.013×10^5 N/m²) and air-flow rates from 0.02 to 0.08 lb/sec (9.07 to 36.3 g/sec) at power inputs from 757 to 1340 kilowatts. Measurements made in three different size supersonic nozzle exits while the tunnel was operated with the above conditions lead to the following conclusions:

1. Stagnation pressures behind the normal shock of 0.03 to 0.72 atm are available.

2. Stagnation-point, cold-wall heating rates on a 1-inch-diameter (2.54-cm) flat-faced probe of 200 to 903 Btu/ft^2-sec (227 to 1025 W/cm^2) are available.

3. Test-stream enthalpies at the stream center line cover a range from 10 000 to 13 000 Btu/lb (23.2 to 30.2 MJ/kg).

4. The test stream is relatively free of strong disturbances and shocks.

5. In the two largest nozzle exits (where profile measurements were made), the profiles of heating rate and pressure are reasonably flat across at least 60 percent of the test stream.

Langley Research Center,
    National Aeronautics and Space Administration,
        Langley Station, Hampton, Va., April 24, 1969,
            124-07-01-47-23.

REFERENCES

1. Mechtly, E. A.: The International System of Units — Physical Constants and Conversion Factors. NASA SP-7012, 1964.

2. Smith, Richard T.; and Kachel, Werner A.: Design and Performance of a High Pressure, Continuous Flow Arc Heater. AFFDL-TR-66-48, U.S. Air Force, May 1966.

3. Gardon, Robert: An Instrument for the Direct Measurement of Intense Thermal Radiation. Rev. Sci. Instr., vol. 24, no. 5, May 1953, pp. 366-370.

4. Fay, J. A.; and Riddell, F. R.: Theory of Stagnation Point Heat Transfer in Dissociated Air. J. Aeronaut. Sci., vol. 25, no. 2, Feb. 1958, pp. 73-85, 121.

5. Holloway, Paul F.; and Dunavant, James C.: Heat-Transfer and Pressure Distributions at Mach Numbers of 6.0 and 9.6 Over Two Reentry Configurations for the Five-Stage Scout Vehicle. NASA TN D-1790, 1963.

6. Beckwith, Ivan E.; and Cohen, Nathaniel B.: Application of Similar Solutions to Calculation of Laminar Heat Transfer on Bodies With Yaw and Large Pressure Gradient in High-Speed Flow. NASA TN D-625, 1961.

7. Zoby, Ernest V.; and Sullivan, Edward M.: Effects of Corner Radius on Stagnation-Point Velocity Gradients on Blunt Axisymmetric Bodies. NASA TM X-1067, 1965.

8. Vojvodich, Nick S.; and Pope, Ronald B.: The Influence of Ablation on Stagnation Region Convective Heating for Dissociated and Partially Ionized Boundary-Layer Flows. Proceedings of the 1965 Heat Transfer and Fluid Mechanics Institute, Andrew F. Charwat, ed., Stanford Univ. Press, c.1965, pp. 114-137.

9. Goulard, R.: On Catalytic Recombination Rates in Hypersonic Stagnation Heat Transfer. Jet Propulsion, vol. 28, no. 11, Nov. 1958, pp. 737-745.

10. Pope, Ronald B.: Measurements of Enthalpy in Low-Density Arc-Heated Flows. AIAA J., vol. 6, no. 1, Jan. 1968, pp. 103-110.

11. Hiester, Nevin K.; and Clark, Carroll F.: Feasibility of Standard Evaluation Procedures for Ablating Materials. NASA CR-379, 1966.

12. Ferri, Antonio; and Zakkay, Victor: Measurements of Stagnation Point Heat Transfer at Low Reynolds Numbers. J. Aerosp. Sci., vol. 29, no. 7, July 1962, pp. 847-850.

13. Lordi, J. A.; Mates, R. E.; and Moselle, J. R.: Computer Program for the Numerical Solution of Nonequilibrium Expansions of Reacting Gas Mixtures. Rep. No. AD-1689-A-6 (Contract No. NASr-109), Cornell Aeron. Lab., Inc., Oct. 1965.

14. Brokaw, R. S.: Energy Transport in High Temperature and Reacting Gases. Planetary Space Sci., vol. 3, 1961, pp. 238-252.

15. Svehla, Roger A.: Estimated Viscosities and Thermal Conductivities of Gases at High Temperatures. NASA TR R-132, 1962.

TABLE I.- SUMMARY OF ARC-HEATER CONDITIONS

Arc-heater condition	Arc-chamber pressure	Air-flow rate		Arc current	Arc voltage	Arc impedance	Arc power	Efficiency
	atm	lb/sec	g/sec	amperes	volts	ohms	kW	percent
1	1.2	0.02	9.07	2620	289	0.113	757	35
2	2.0	.04	18.1	2600	381	.147	991	41
3	3.3	.08	36.3	2310	578	.250	1340	51

TABLE II.- TEST-STREAM CENTER-LINE MEASUREMENTS OF

STAGNATION-POINT HEATING RATE[a] AND PRESSURE

IN THE 1.00-INCH-RADIUS (2.54-cm) NOZZLE

x	$\dot{q}$		$p_{t,2}$
	$\dfrac{\text{Btu}}{\text{ft}^2\text{-sec}}$	$\dfrac{\text{W}}{\text{cm}^2}$	atm
Arc-heater condition 1			
$0.4R_E$	760	862	0.280
$.8R_E$	714	810	.249
$1.2R_E$	657	745	.225
Arc-heater condition 2			
$0.4R_E$	854	967	0.434
$.8R_E$	840	952	.392
$1.2R_E$	773	876	.346
Arc-heater condition 3			
$0.4R_E$	903	1025	0.720
$.8R_E$	869	985	.634
$1.2R_E$	834	945	.589

[a]Heating-rate values are for a 1-inch-diameter (2.54-cm)
flat-faced probe measured with the transient heat-transfer probe.

TABLE III.- SOME CALCULATED CONDITIONS[a] FOR THE HIGH-ENTHALPY ARC TUNNEL FOR THREE DIFFERENT NOZZLE EXITS

(a) U.S. Customary Units

$p_{t,1}$, atm (b,c)	M	H_t, $\frac{Btu}{lb}$	V_∞, $\frac{ft}{sec}$	ρ_∞, $\frac{slugs}{ft^3}$	p_∞, $\frac{lb}{ft^2}$	T_∞, °R	$N_{Re,\infty}$, ft^{-1}	μ_∞, $\frac{lb\text{-}sec}{ft^2}$	Mole fraction of primary constituents			
									N	N_2	O	Ar
$R_E = 1.00$ in.[b]; $A/A_{min} = 7.12$[b]; $T_t = 13\,000°$ R[c]												
1.2	3.78	11 970	13 580	28.6×10^{-7}	23.8	3070	3.28×10^4	1.183×10^{-6}	0.508	0.227	0.259	0.006
2.0	3.60	10 890	13 480	48.1	45.7	3600	4.90	1.321	.427	.293	.273	.006
3.3	3.44	9 880	13 420	80.9	86.1	4270	7.31	1.486	.339	.366	.288	.006
$R_E = 2.30$ in.[b]; $A/A_{min} = 37.7$[b]; $T_t = 13\,000°$ R[c]												
1.2	6.38	11 970	14 630	4.86×10^{-7}	1.67	1230	1.09×10^4	0.653×10^{-6}	0.508	0.227	0.259	0.006
2.0	5.94	10 890	14 670	8.26	3.34	1530	1.60	.757	.426	.294	.273	.006
3.3	5.55	9 880	14 790	13.90	6.74	1925	2.32	.884	.337	.368	.288	.006
$R_E = 3.82$ in.[b]; $A/A_{min} = 104$[b]; $T_t = 13\,000°$ R[c]												
1.2	8.61	11 970	14 930	1.73×10^{-7}	0.337	699	0.642×10^4	0.402×10^{-6}	0.507	0.228	0.259	0.006
2.0	7.91	10 890	15 000	2.92	.689	892	.827	.523	.426	.295	.273	.006
3.3	7.27	9 880	15 180	4.91	1.421	1163	1.170	.636	.337	.368	.288	.006

[a]Conditions calculated by assuming nonequilibrium flow.

[b]Measured quantity.

[c]Input to computer program.

TABLE III.- SOME CALCULATED CONDITIONS[a] FOR THE HIGH-ENTHALPY ARC TUNNEL FOR THREE DIFFERENT NOZZLE EXITS – Concluded

(b) SI Units

$p_{t,1}$, atm (b,c)	M	H_t, $\frac{MJ}{kg}$	V_∞, $\frac{m}{sec}$	ρ_∞, $\frac{g}{m^3}$	p_∞, $\frac{N}{m^2}$	T_∞, °K	$N_{Re,\infty}$, m^{-1}	μ_∞, $\frac{N\text{-sec}}{m^2}$	Mole fraction of primary constituents			
									N	N_2	O	Ar
						$R_E = 2.54$ cm [b]; $A/A_{min} = 7.12$ [b]; $T_t = 7200°$ K [c]						
1.2	3.78	27.8	4140	1.47	1040	1710	10.75×10^4	56.6×10^{-6}	0.508	0.227	0.259	0.006
2.0	3.60	25.3	4110	2.48	2190	2000	16.08	63.3	.427	.293	.273	.006
3.3	3.44	22.9	4090	4.17	4125	2870	24.00	71.1	.339	.366	.288	.006
						$R_E = 5.84$ cm [b]; $A/A_{min} = 37.7$ [b]; $T_t = 7200°$ K [c]						
1.2	6.38	27.8	4460	0.250	80	684	3.58×10^4	31.3×10^{-6}	0.508	0.227	0.259	0.006
2.0	5.94	25.3	4470	.426	160	850	5.25	36.2	.426	.294	.273	.006
3.3	5.55	22.9	4510	.716	323	1070	7.61	42.3	.337	.368	.288	.006
						$R_E = 9.7$ cm [b]; $A/A_{min} = 104$ [b]; $T_t = 7200°$ K [c]						
1.2	8.61	27.8	4550	0.089	16	388	2.11×10^4	19.2×10^{-6}	0.507	0.228	0.259	0.006
2.0	7.91	25.3	4570	.151	33	495	2.72	25.0	.426	.295	.273	.006
3.3	7.27	22.9	4630	.253	68	646	3.84	30.5	.337	.368	.288	.006

[a]Conditions calculated by assuming nonequilibrium flow.

[b]Measured quantity.

[c]Input to computer program.

Station	Nozzle-exit radius	
①	1.00 in.	2.54 cm
②	2.30 in.	5.84 cm
③	3.82 in.	9.70 cm
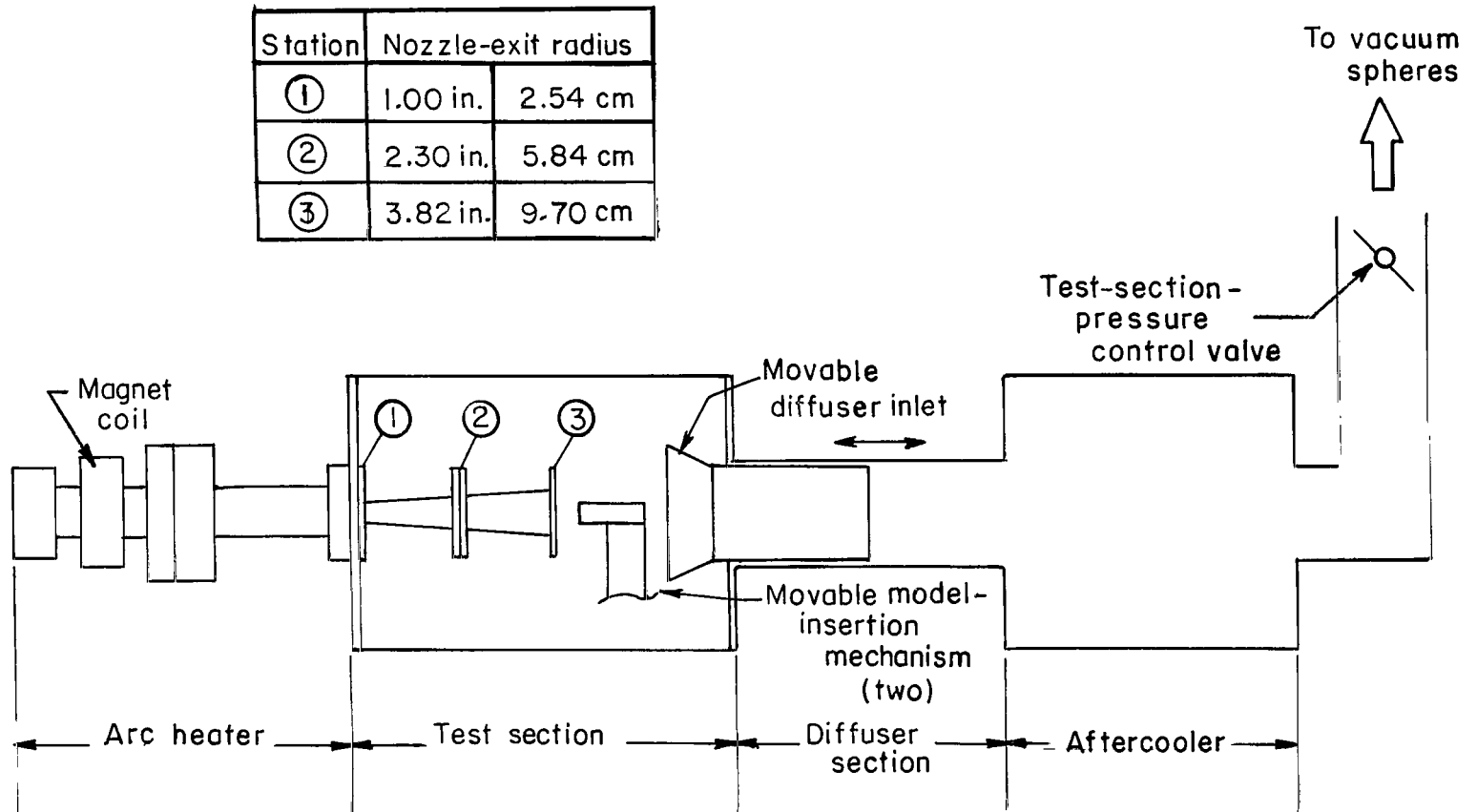
Figure 1.- Overall schematic view of the high-enthalpy arc tunnel at the Langley Research Center.
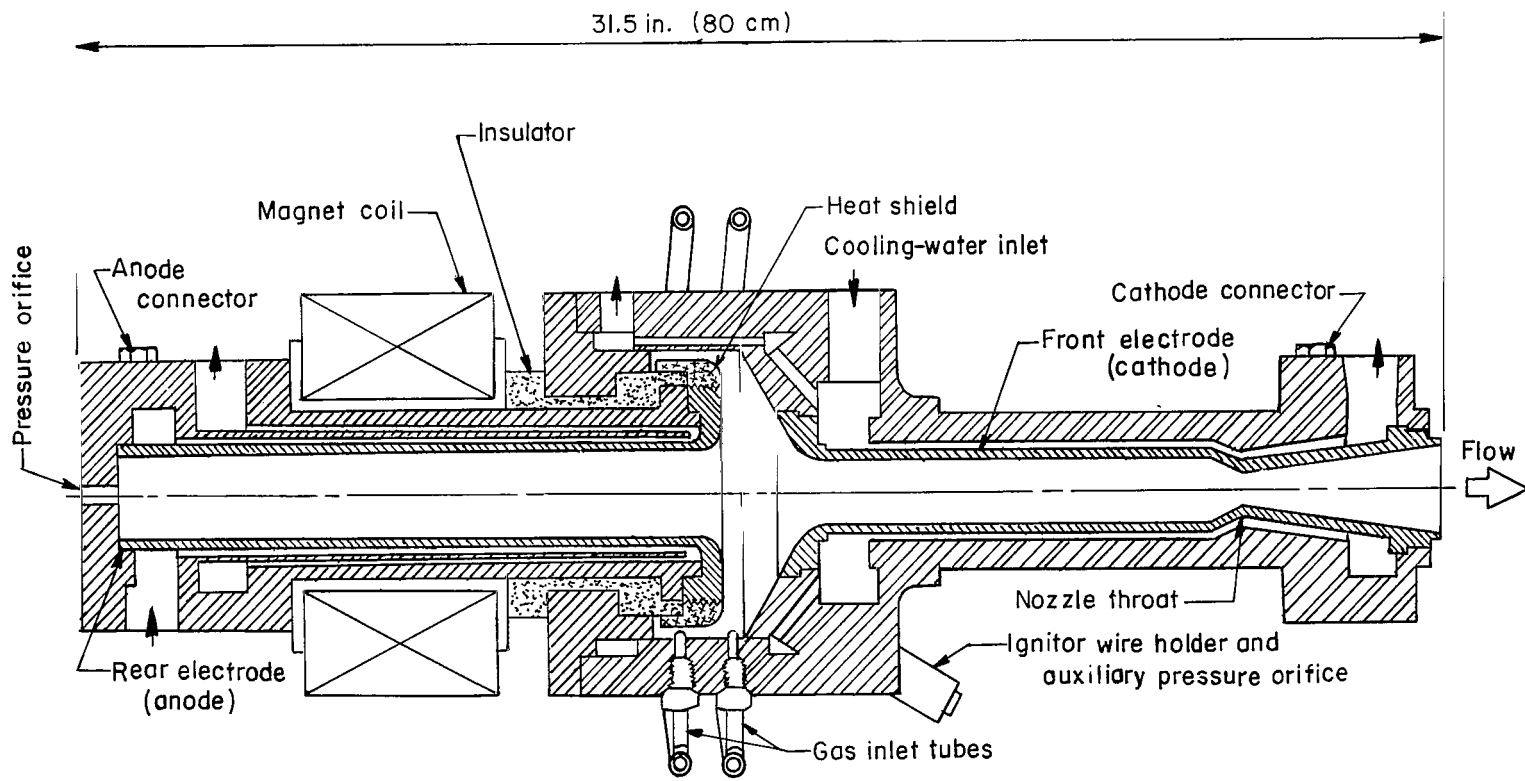
Figure 2.- Simplified cross-sectional view of arc heater.

Transfer switch

Ballast resistor bank

Circuit breaker

1500-volt
battery bank

Arc-voltage -
measuring circuit

Electrodes

Current-
measuring shunt

Battery
charger

Magnet coil

Circuit
breaker

Transfer
switch

125-volt battery bank

Battery
charger
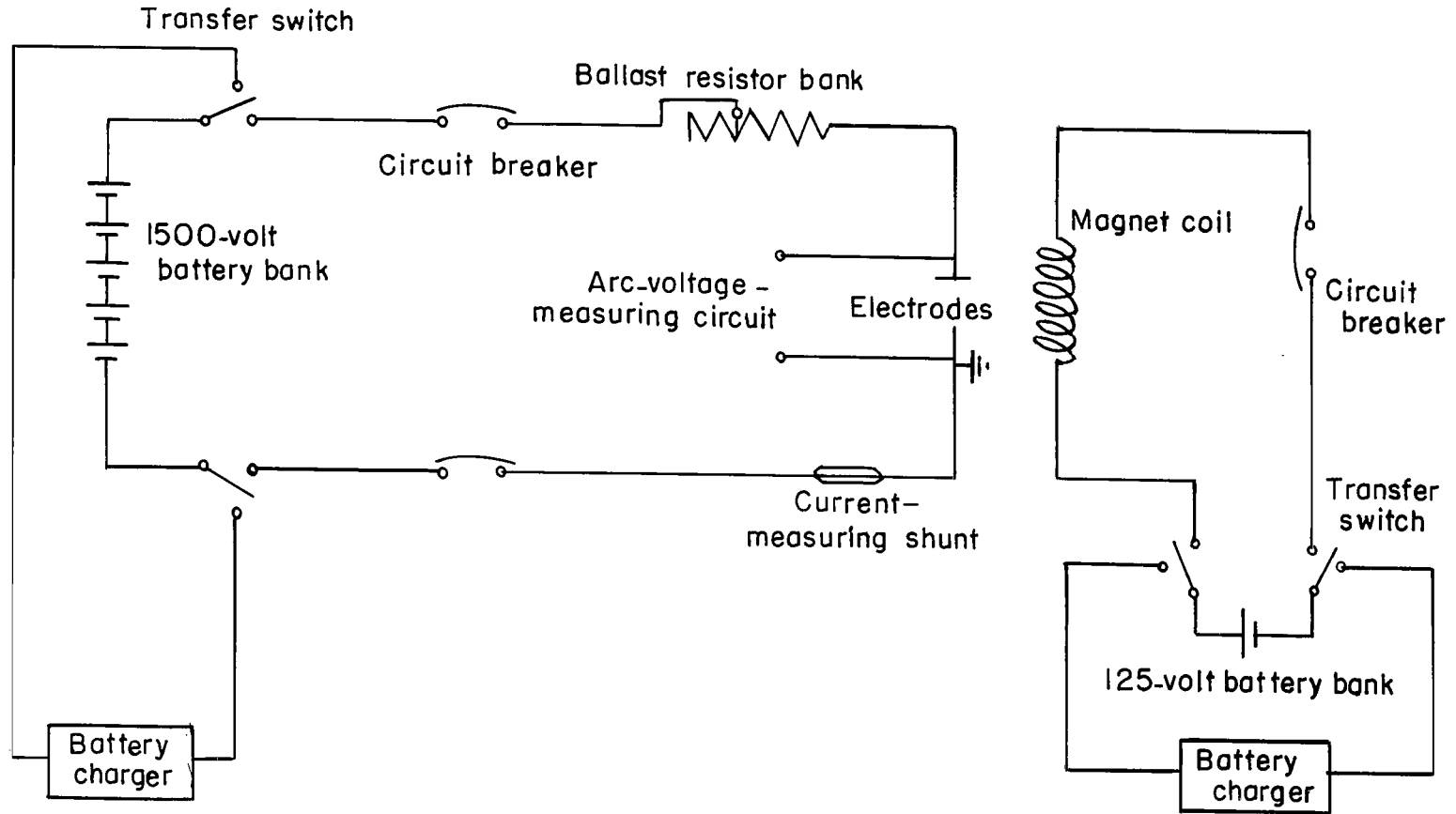
Figure 3.- Electrical circuit diagram for arc heater and magnet coil.
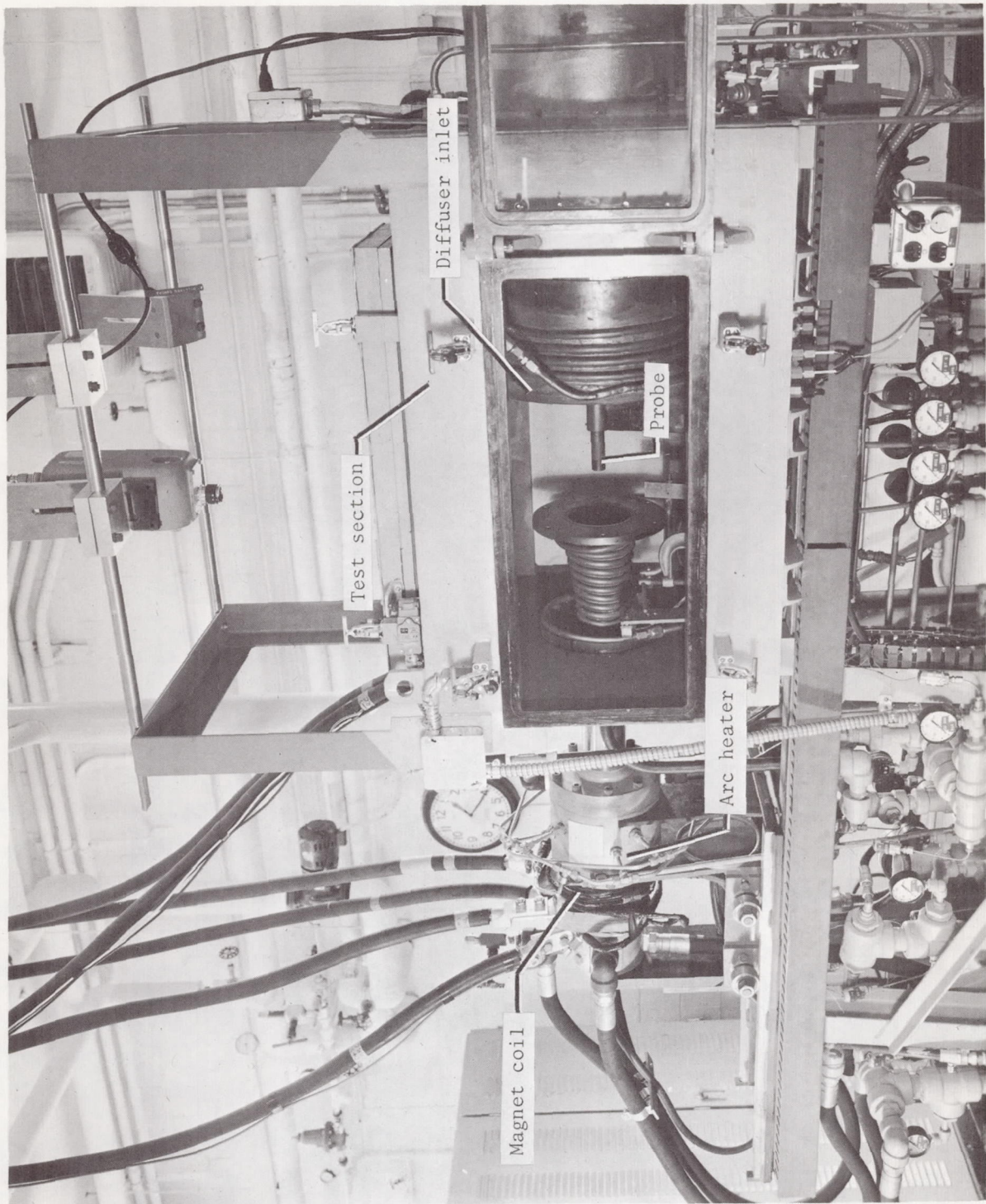
Figure 4.- Overall view of arc heater and test section.

L-66-9399.1

23
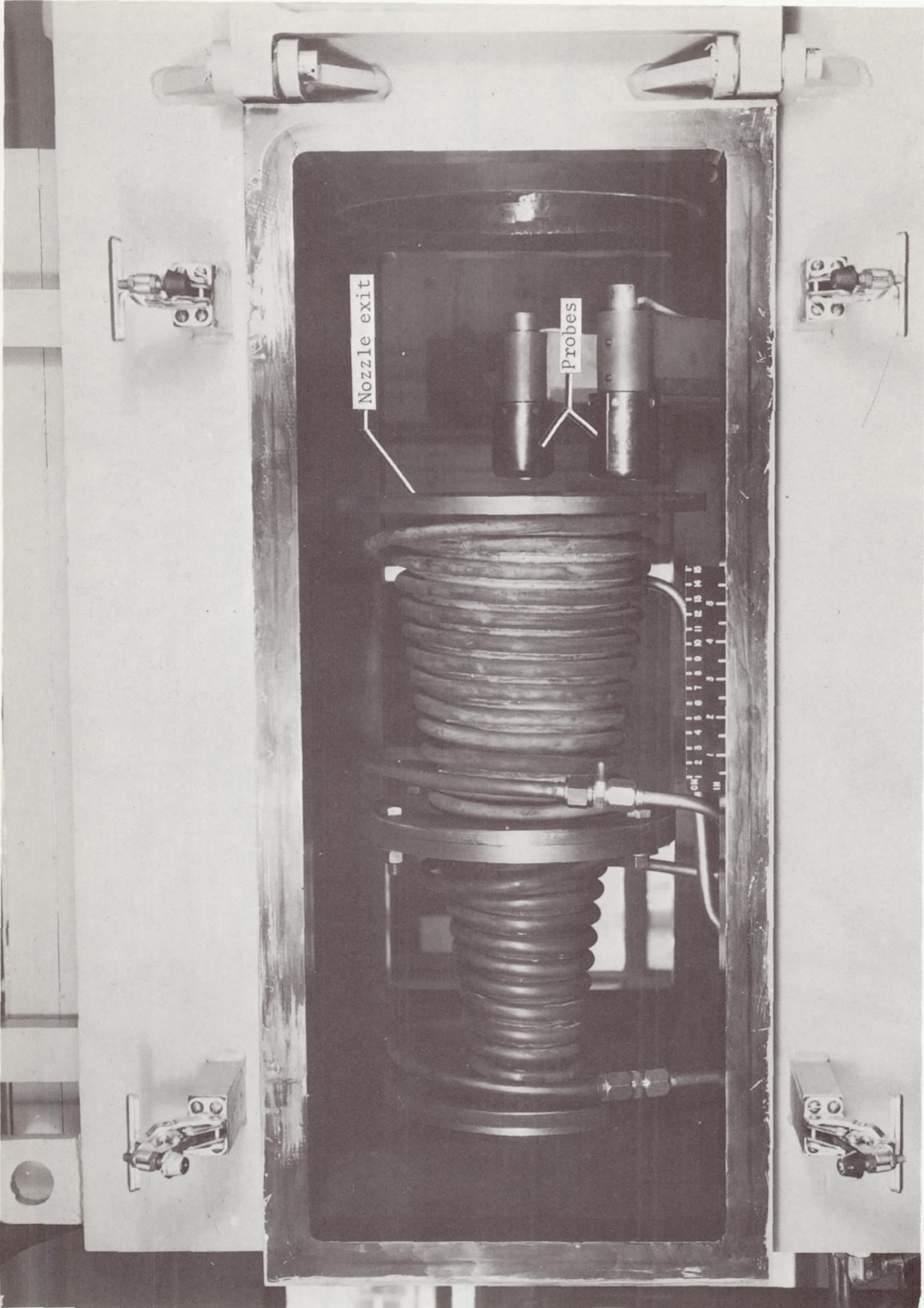
(a) 3.82-inch-radius (9.70-cm) nozzle exit.

Figure 5.- View of test section.

L-66-2493.1

24
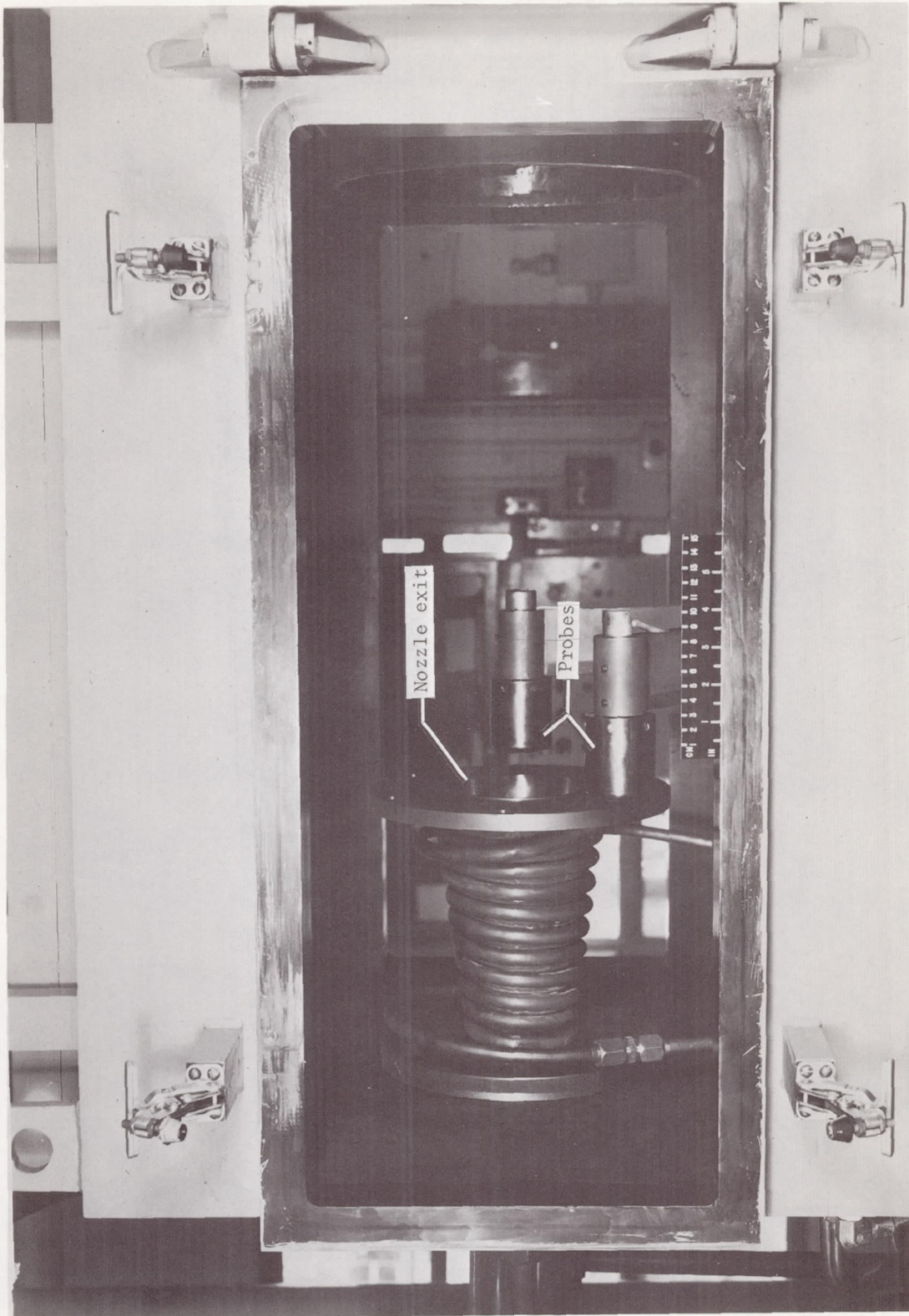
(b) 2.30-inch-radius (5.84-cm) nozzle exit.

Figure 5.- Continued.
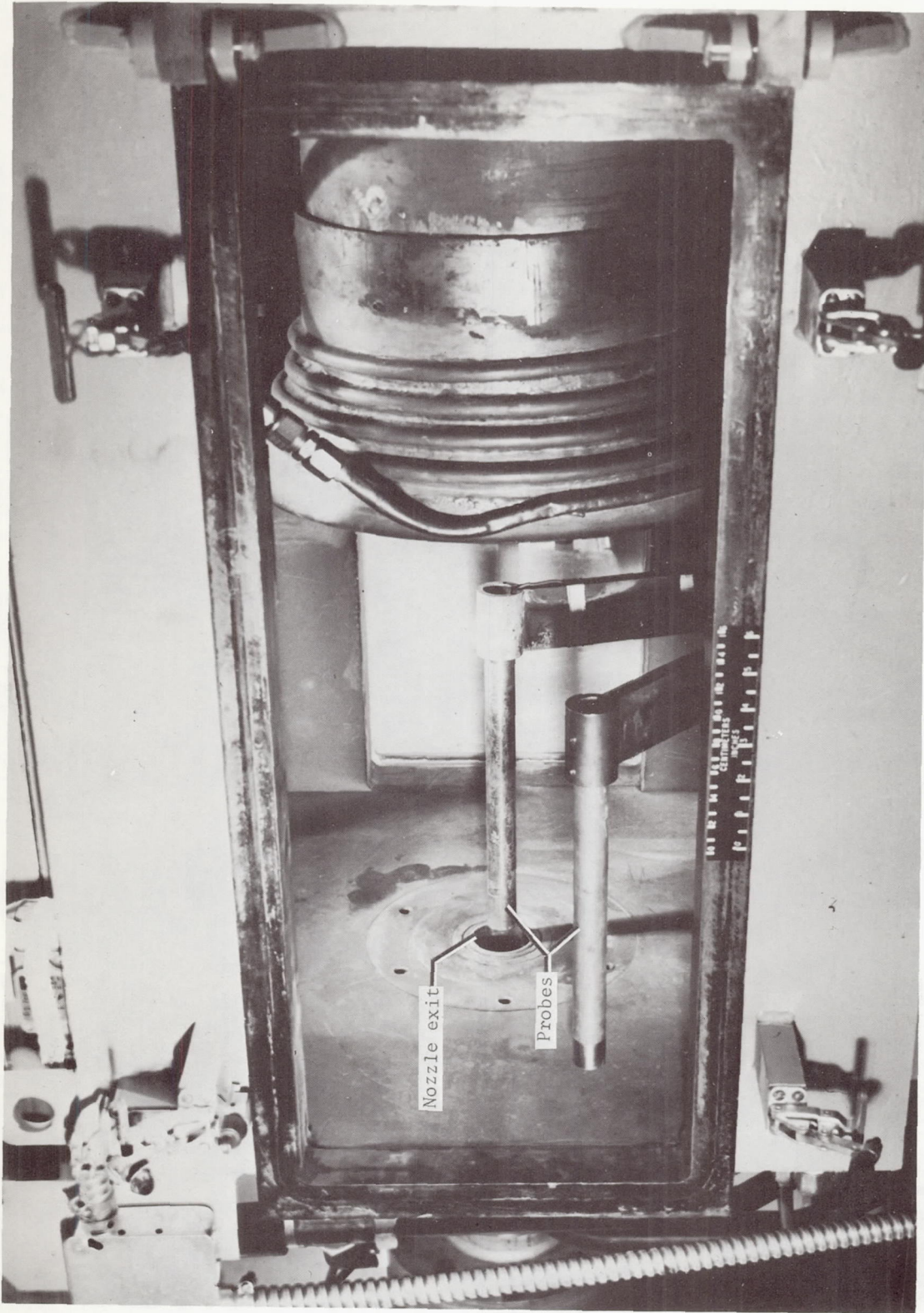
(c) 1.00-inch-radius (2.54-cm) nozzle exit.

Figure 5.- Concluded.

diam = 1 in. (2.54 cm)

Water tubes

Copper leads

Constantan-foil sensing area

(a) Steady-state heat-transfer probe.

diam = 1 in. (2.54 cm)

Thermocouple leads

Stainless-steel thin wall
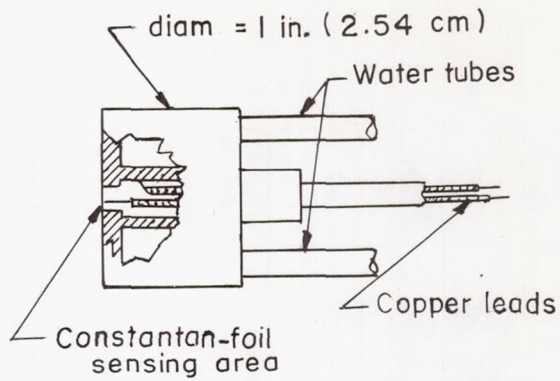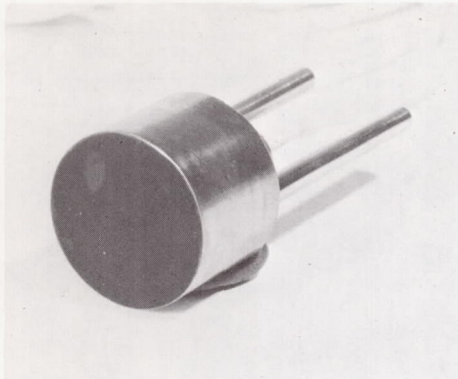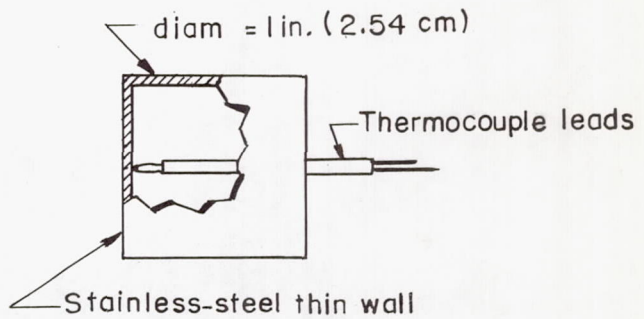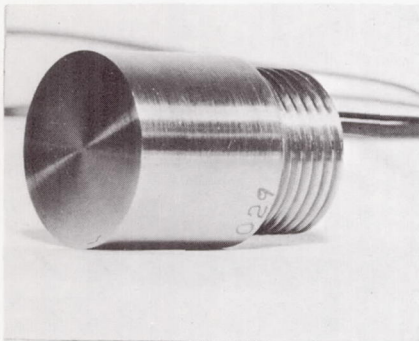
(b) Transient heat-transfer probe.
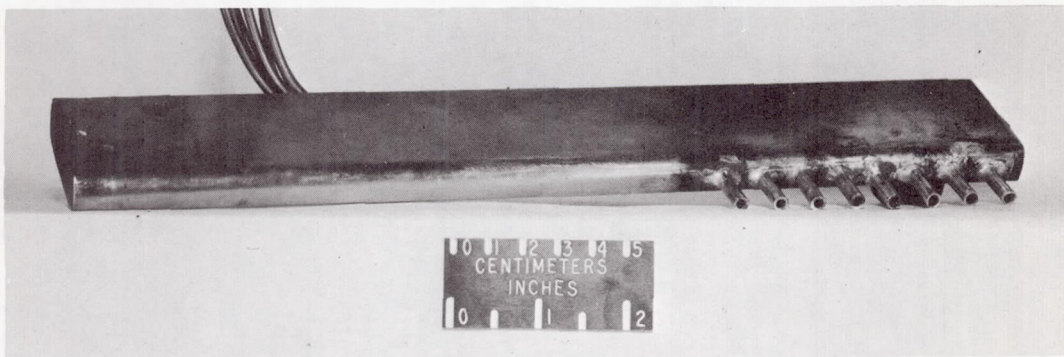
(c) Pressure rake.

Figure 6.- Probes used for test-stream measurements.
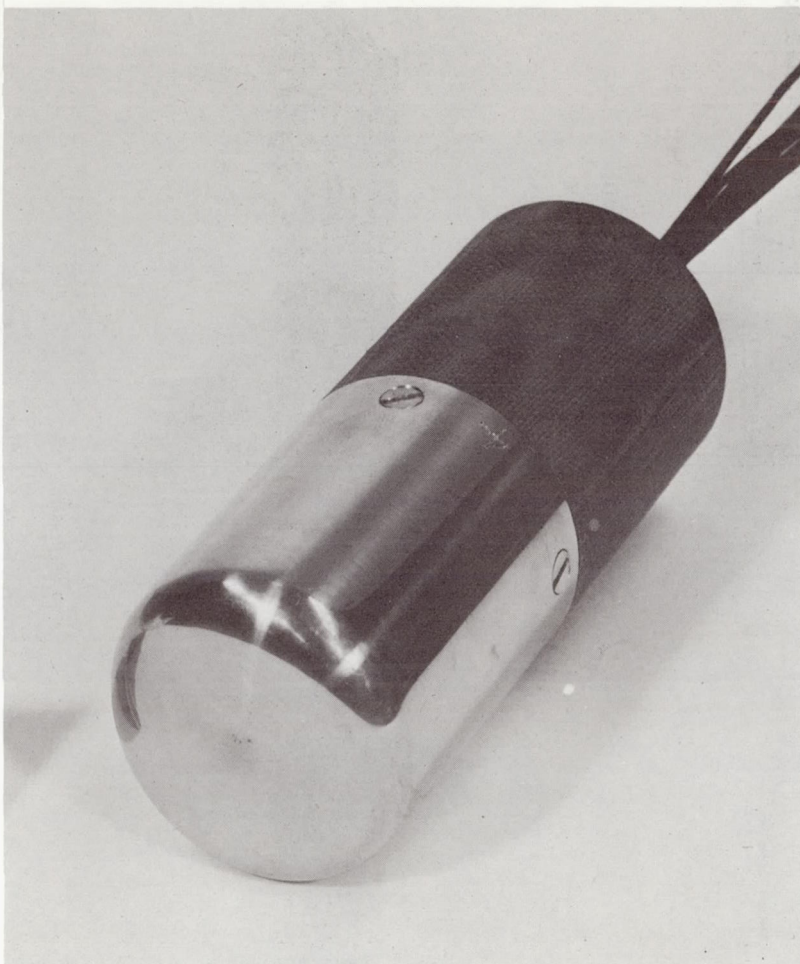
Point	S/R_B
①	0
②	.41
③	.61
④	.83
⑤	1.18
⑥	1.56
⑦	2.06
⑧	2.54

Nominal wall thickness = 0.050 in. (0.127 cm)

R_B = 0.75 in. (1.91 cm)

R_n = 2.355 in. (5.98 cm)

R_c = 0.21 in. (0.53 cm)
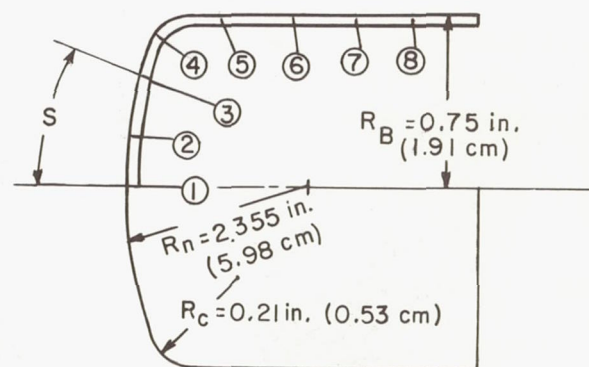
Figure 7.- Transient heat-transfer distribution probe.

L-66-8137
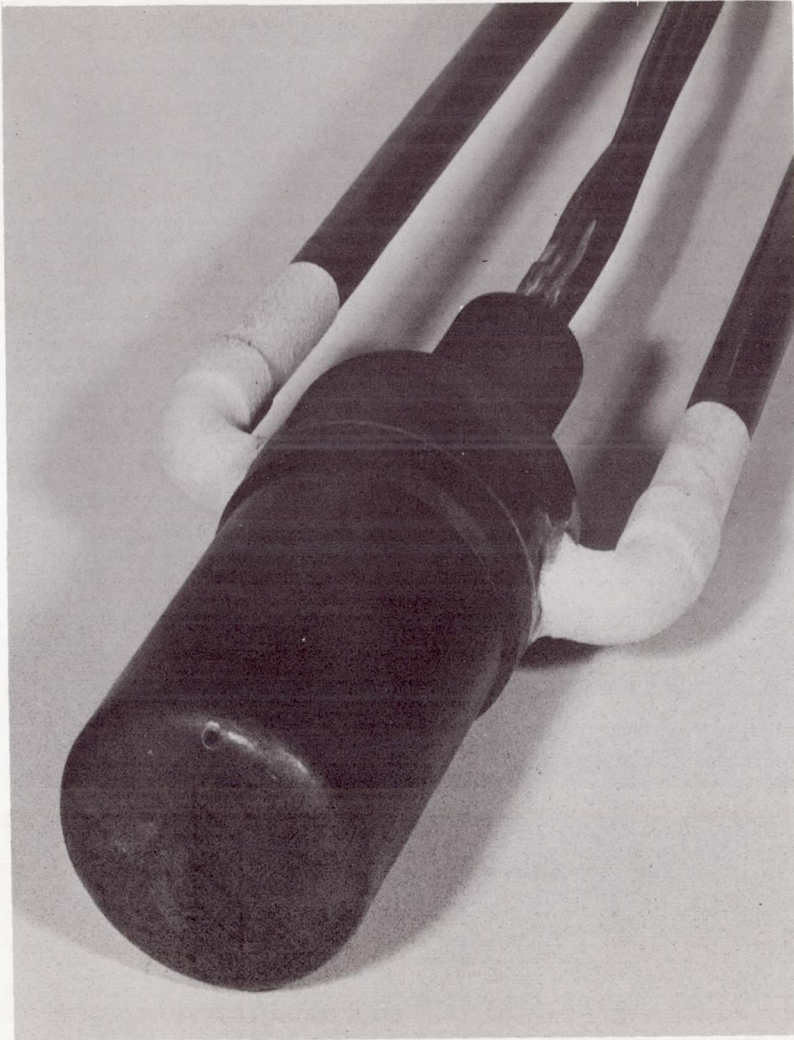
Point	S/R_B
①	0
②	.41
③	.71
④	.85
⑤	1.07
⑥	1.48

$R_B = 0.75$ in. (1.91 cm)

$R_n = 2.355$ in. (5.98 cm)

$R_c = 0.21$ in. (0.53 cm)
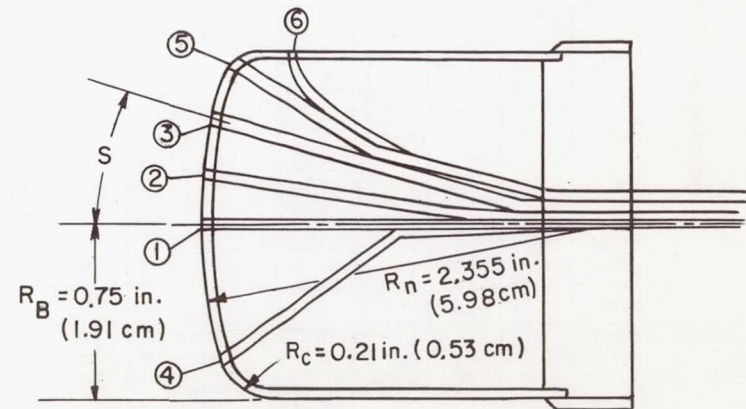
Figure 8.- Pressure-distribution probe.

L-66-8140
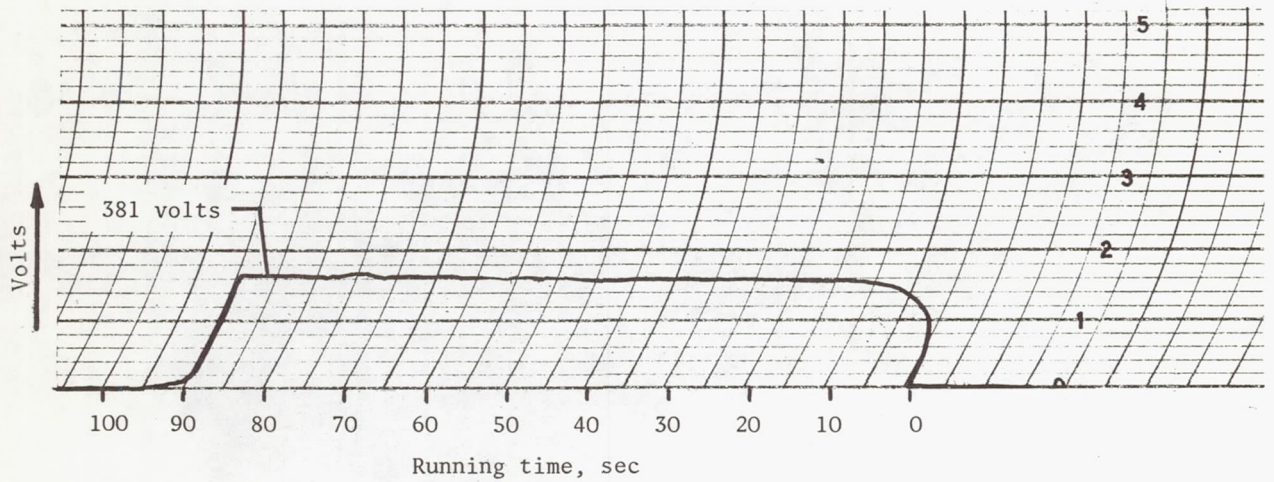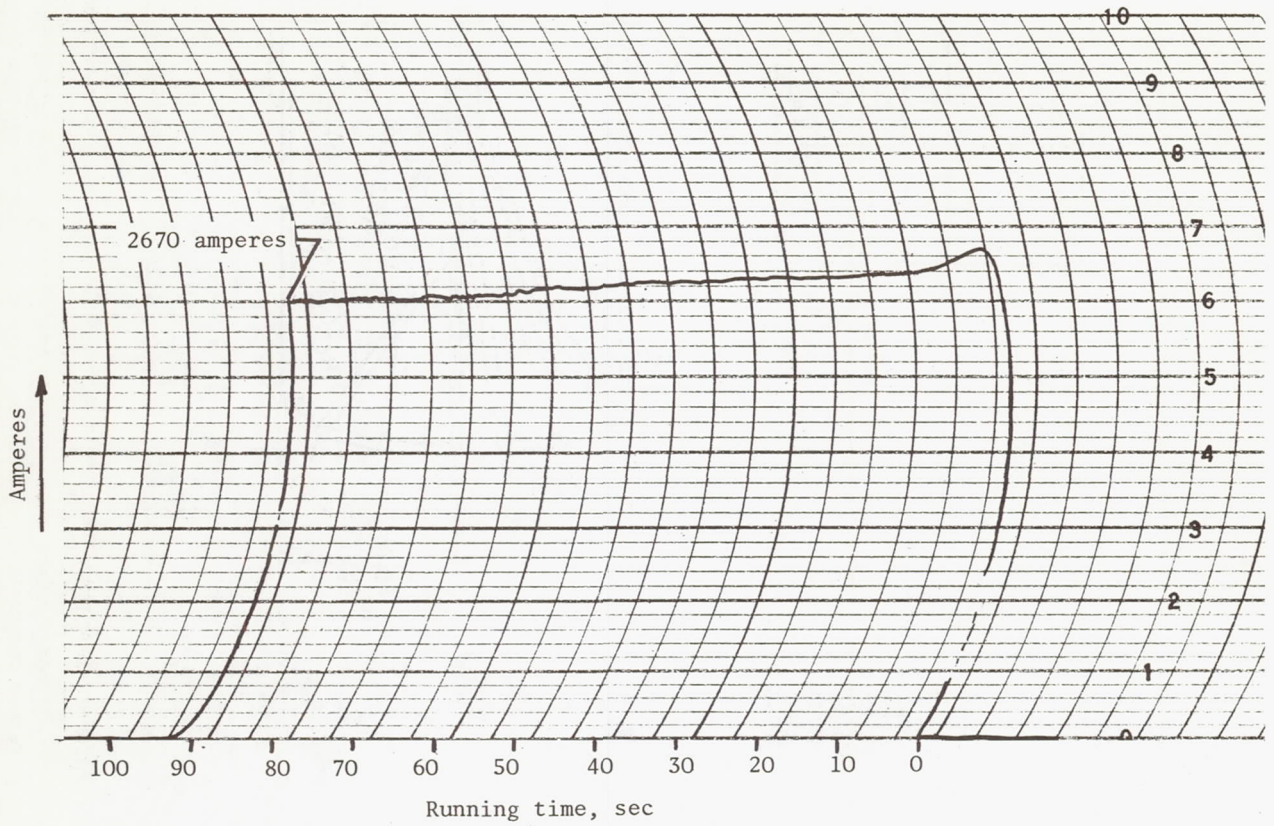
Figure 9.- Typical traces from a strip-chart recorder for arc current and voltage at arc-chamber pressure of 2.0 atm.

30

Arcing surface

Cooling-water side
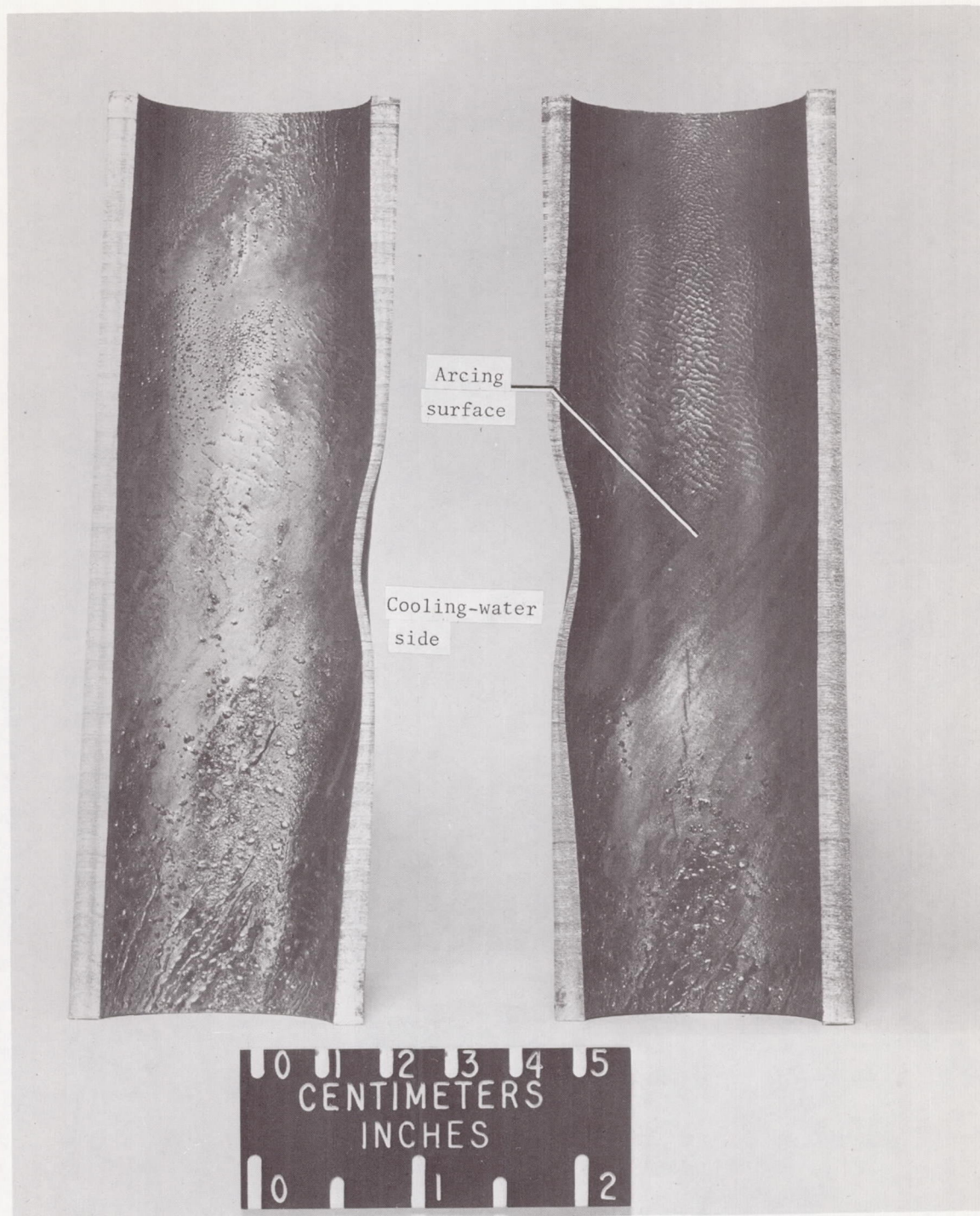
Figure 10.- Sectioned part of front electrode (cathode) in arc attachment area.

L-67-8984.1

Original shape of section

Arcing surface

Cooling-water side
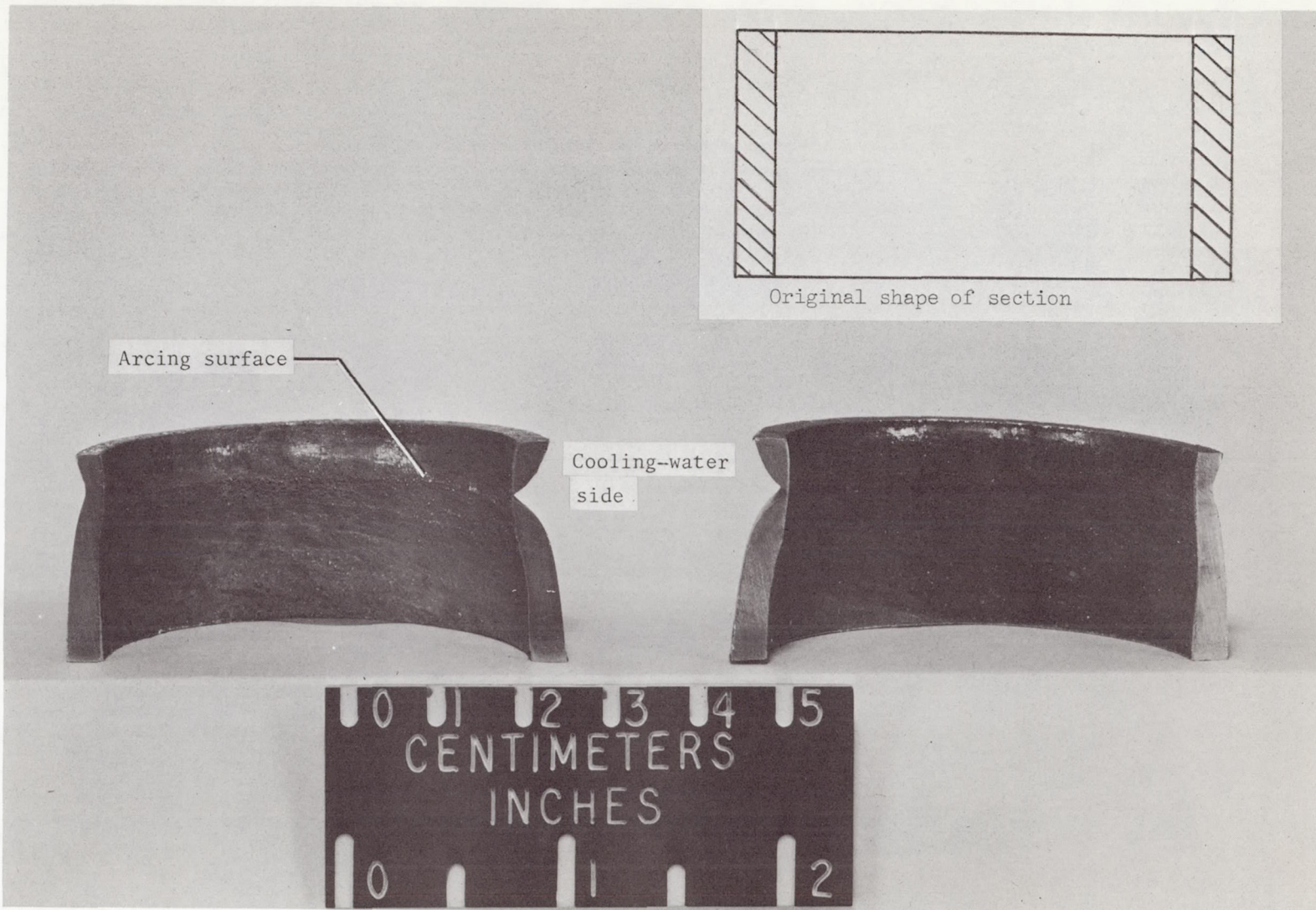
Figure 11.- Sectioned part of rear electrode (anode) in arc attachment area.

L-67-8983.1

Crack

Arc attachment area in rear electrode
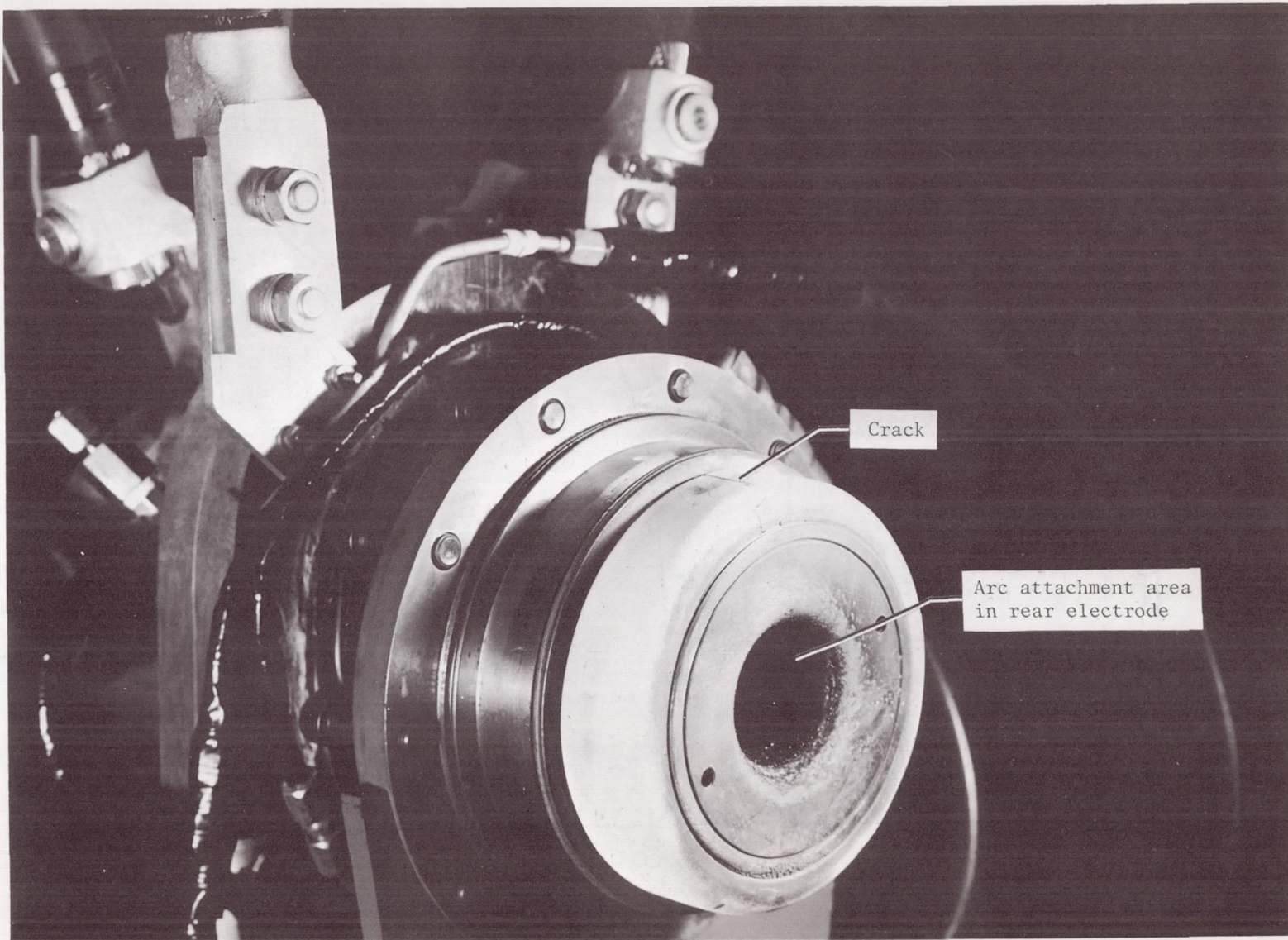
Figure 12.- View of boron-nitride heat shield with initial crack.

L-66-9878.1
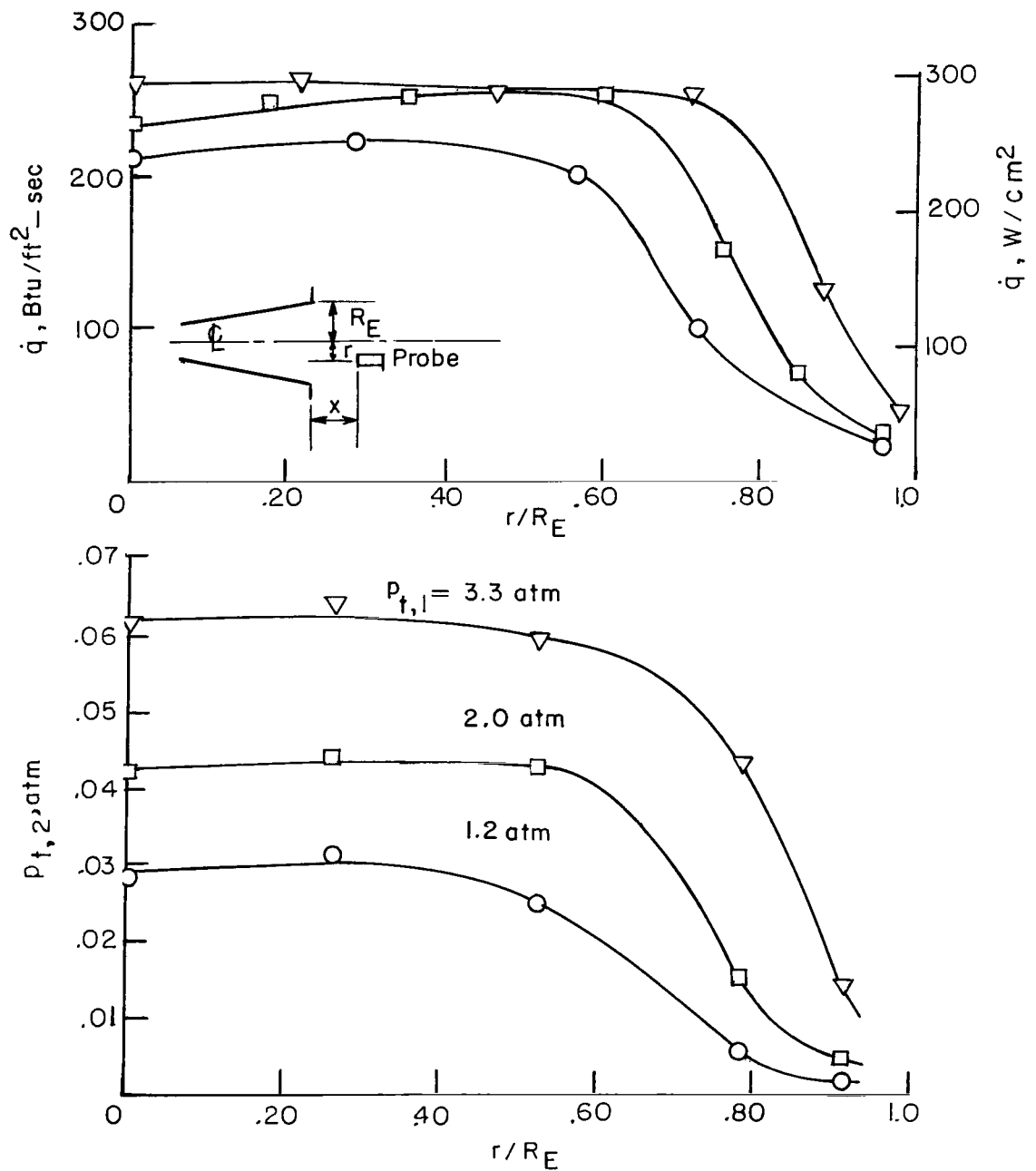
(a) x = 0.4R_E.

Figure 13.- Distribution of $\dot{q}$ and $p_{t,2}$ across test stream for R_E = 3.82 inches (9.70 cm). Values of $\dot{q}$ are for a 1-inch-diameter (2.54-cm) flat-faced probe.
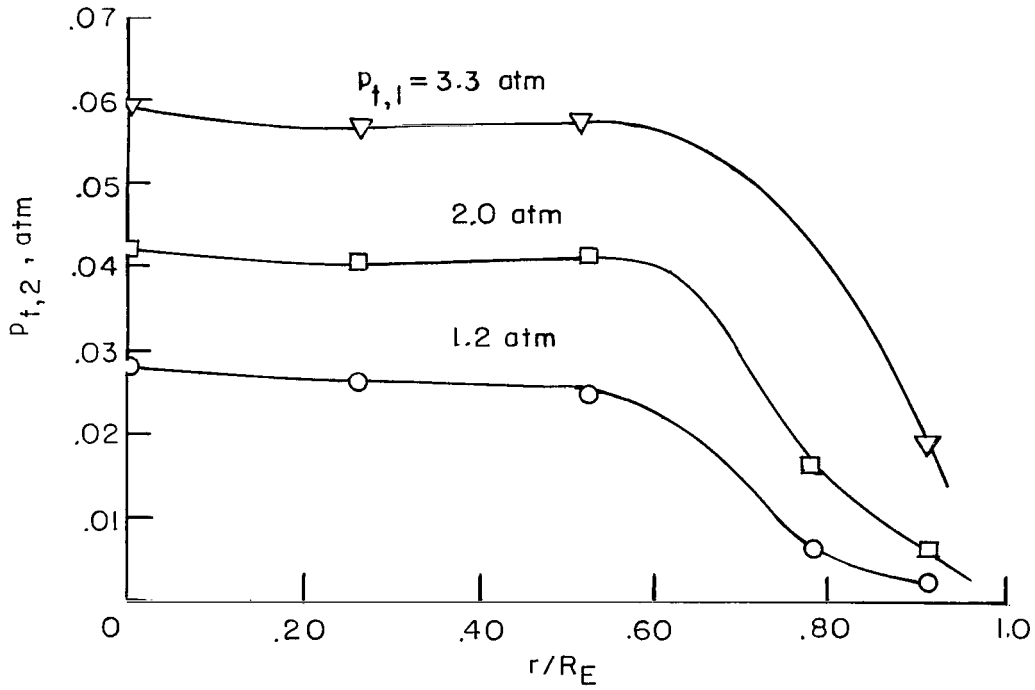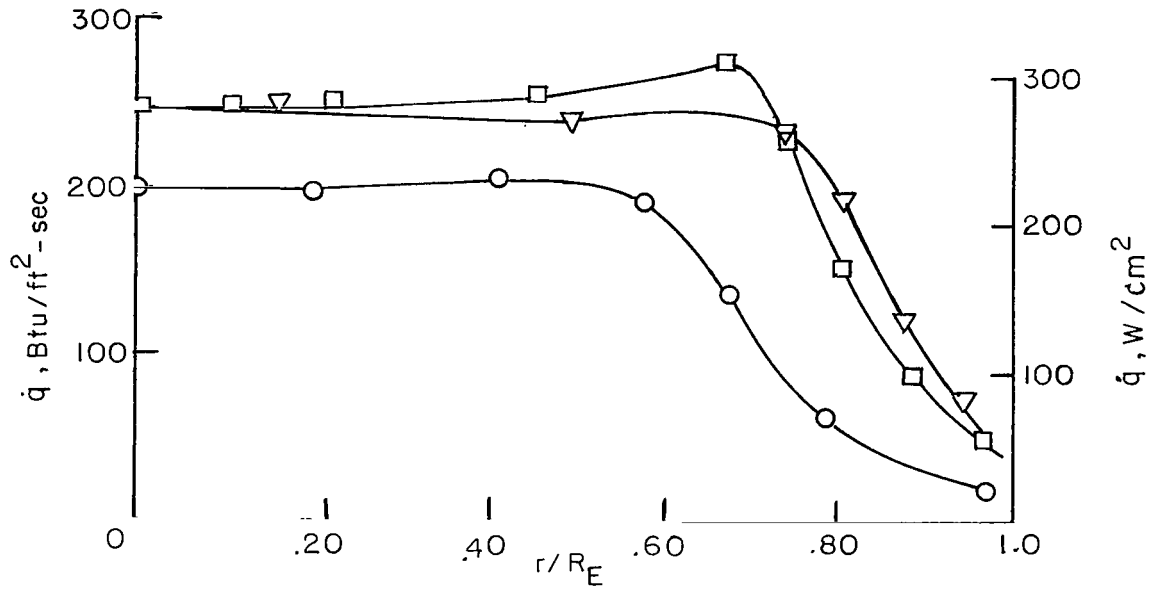
(b) x = 0.8R_E.

Figure 13.- Continued.
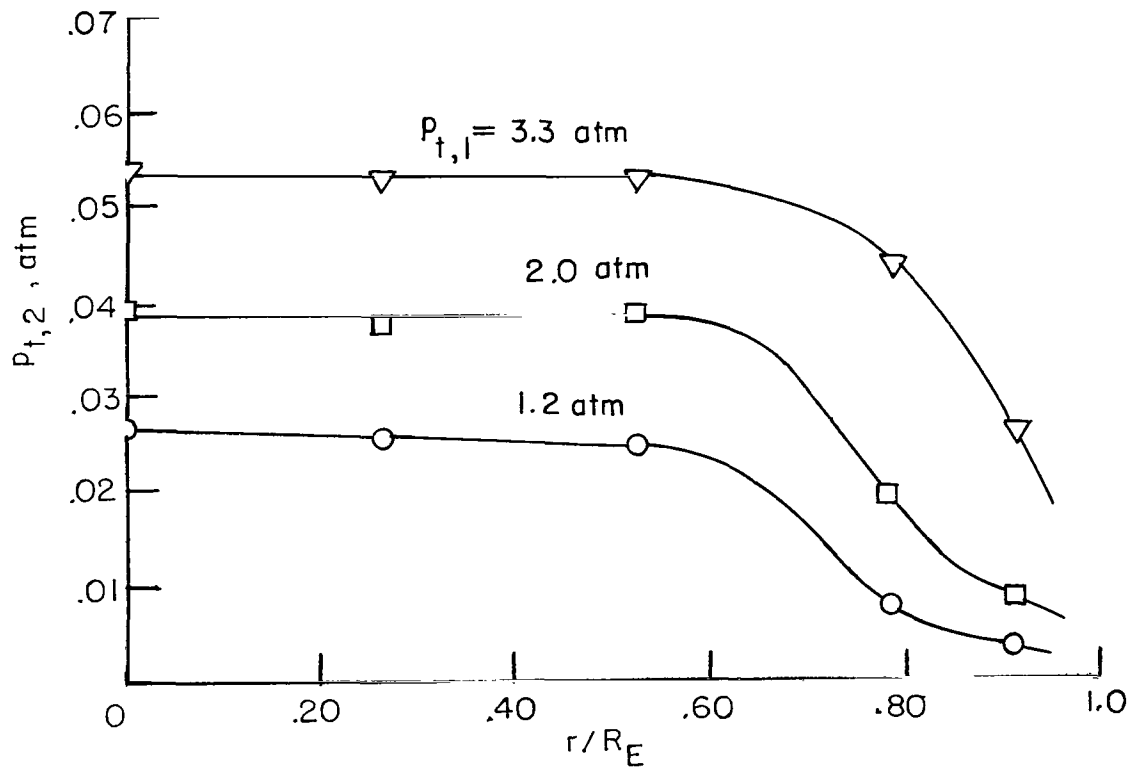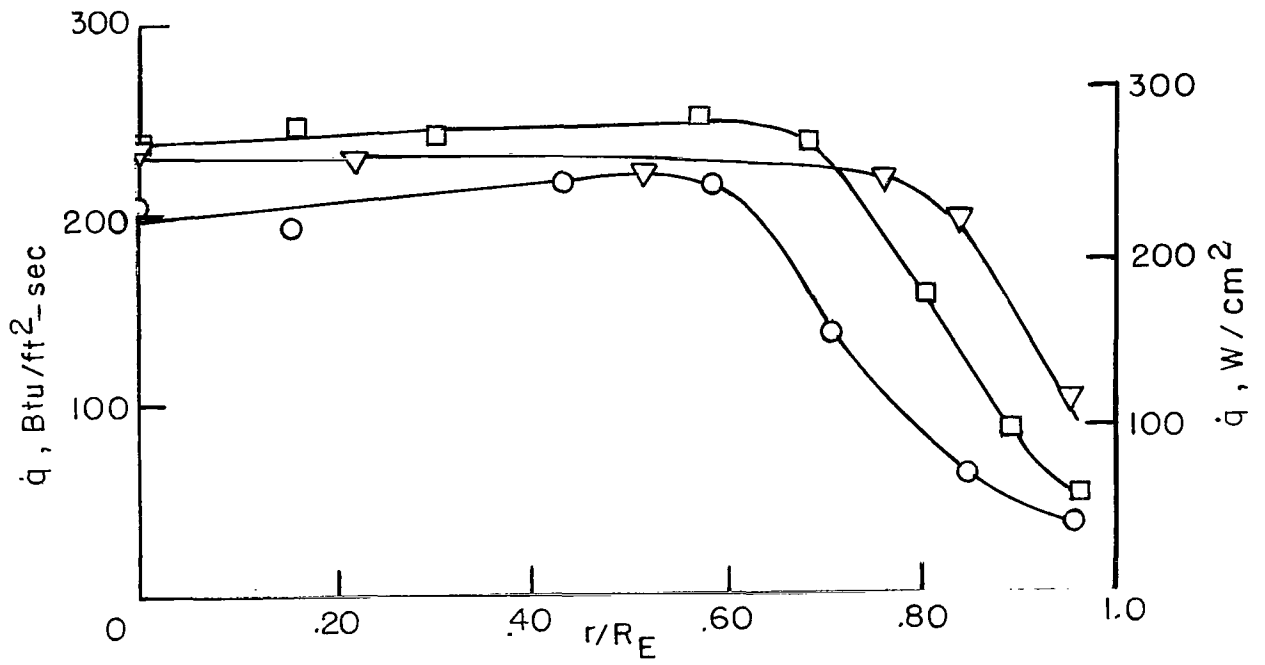
(c) $x = 1.2R_E$.

Figure 13.- Concluded.
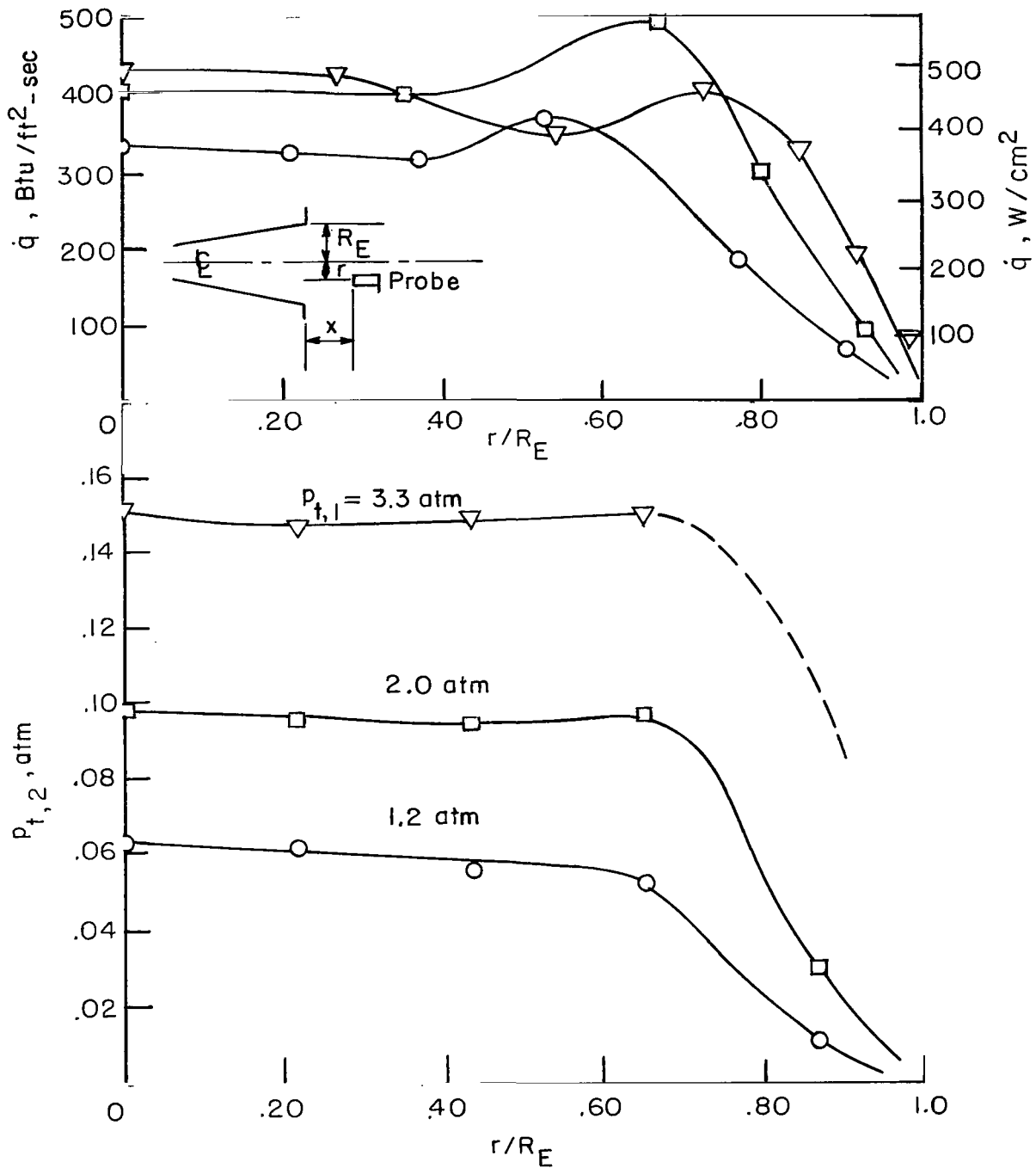
Figure 14.- Distribution of $\dot{q}$ and $p_{t,2}$ across test stream for R_E = 2.30 inches (5.84 cm). Values of $\dot{q}$ are for a 1-inch-diameter (2.54-cm) flat-faced probe.

(a) $x = 0.4R_E$.
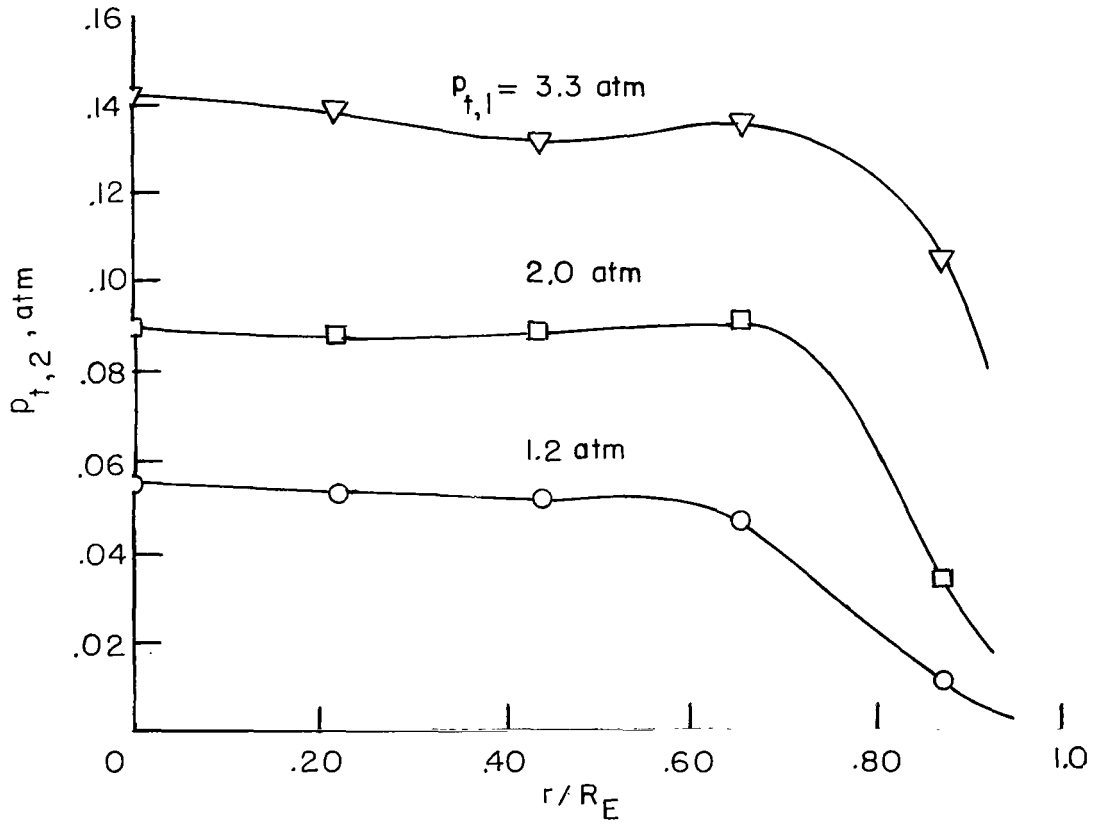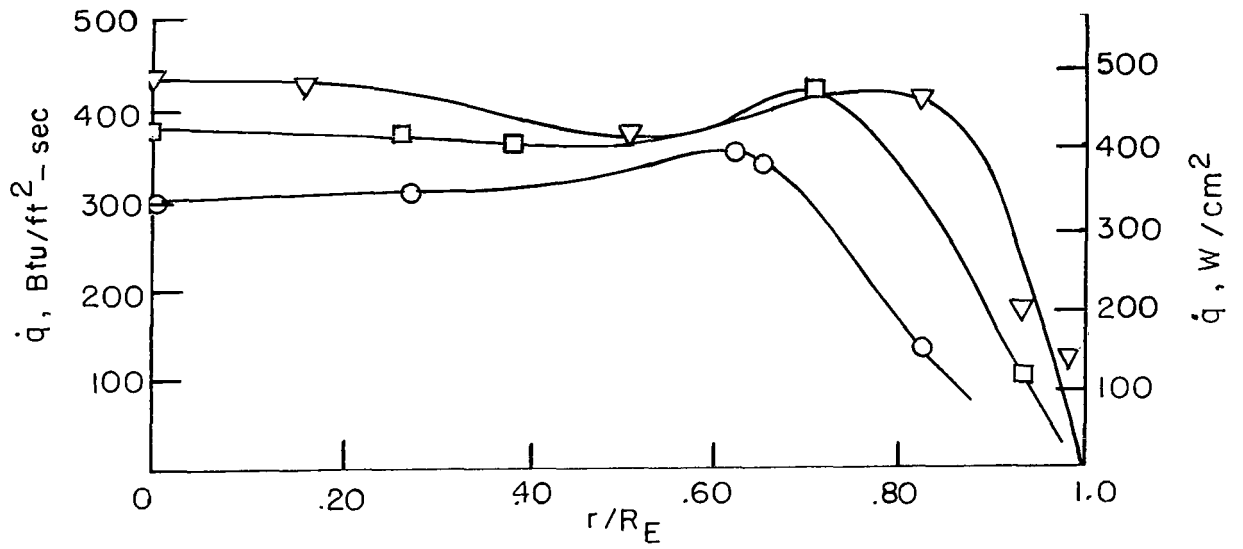
(b) x = 0.8R_E.

Figure 14.- Continued.
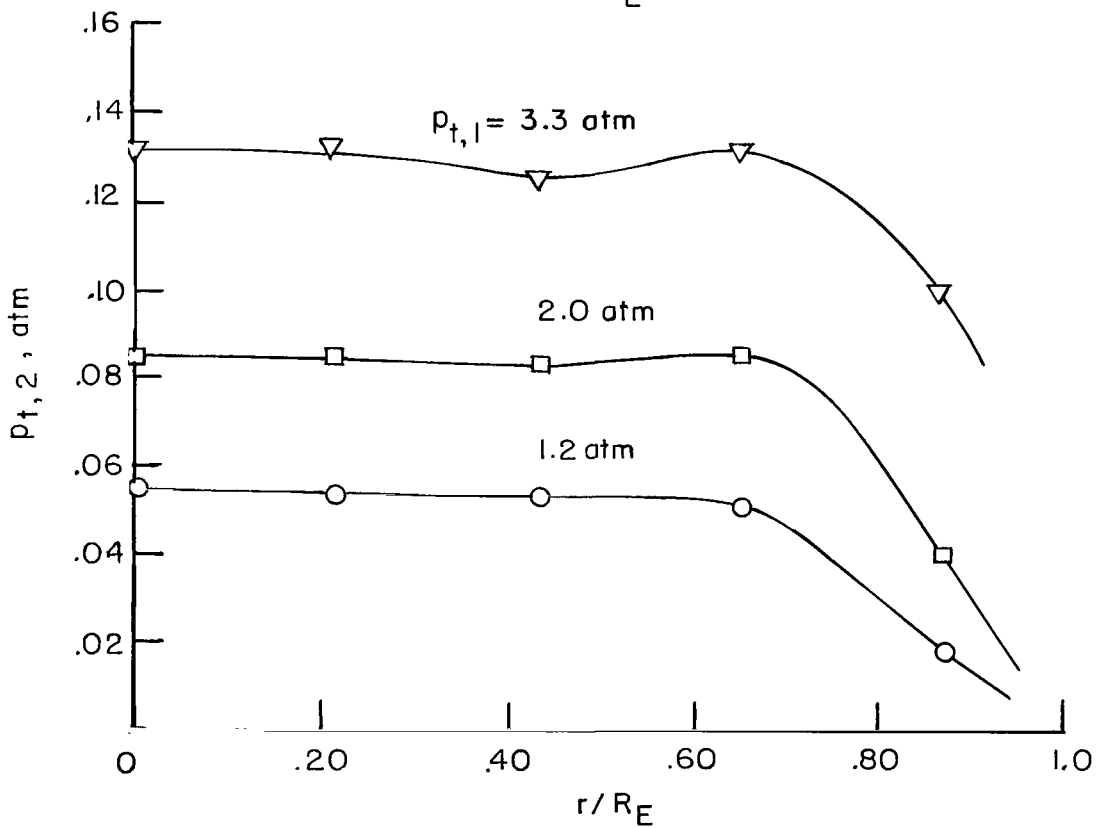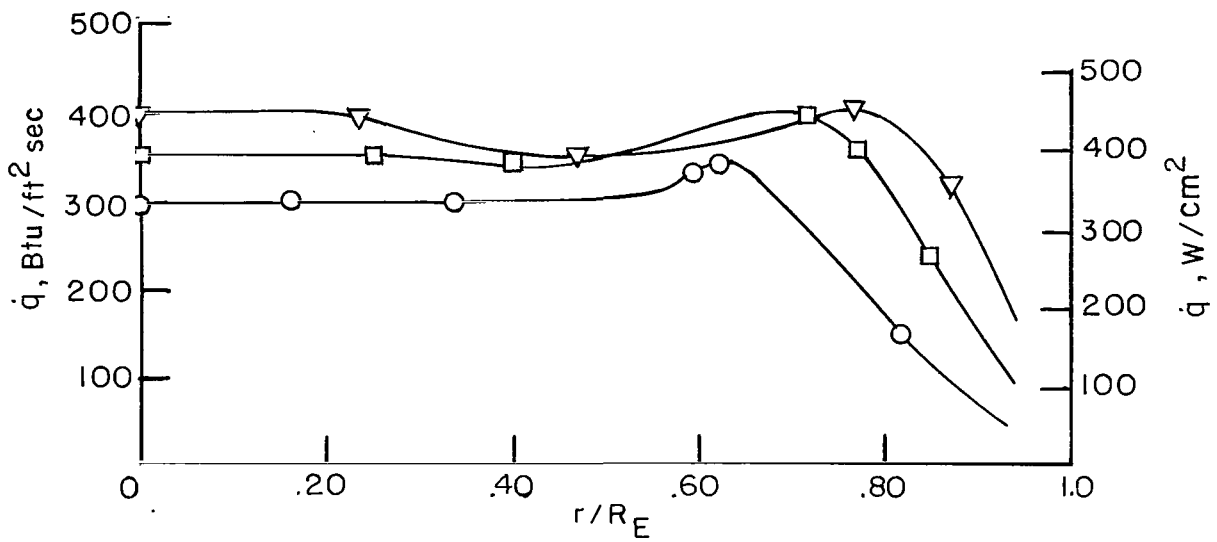
(c) $x = 1.2R_E$.

Figure 14.- Concluded.
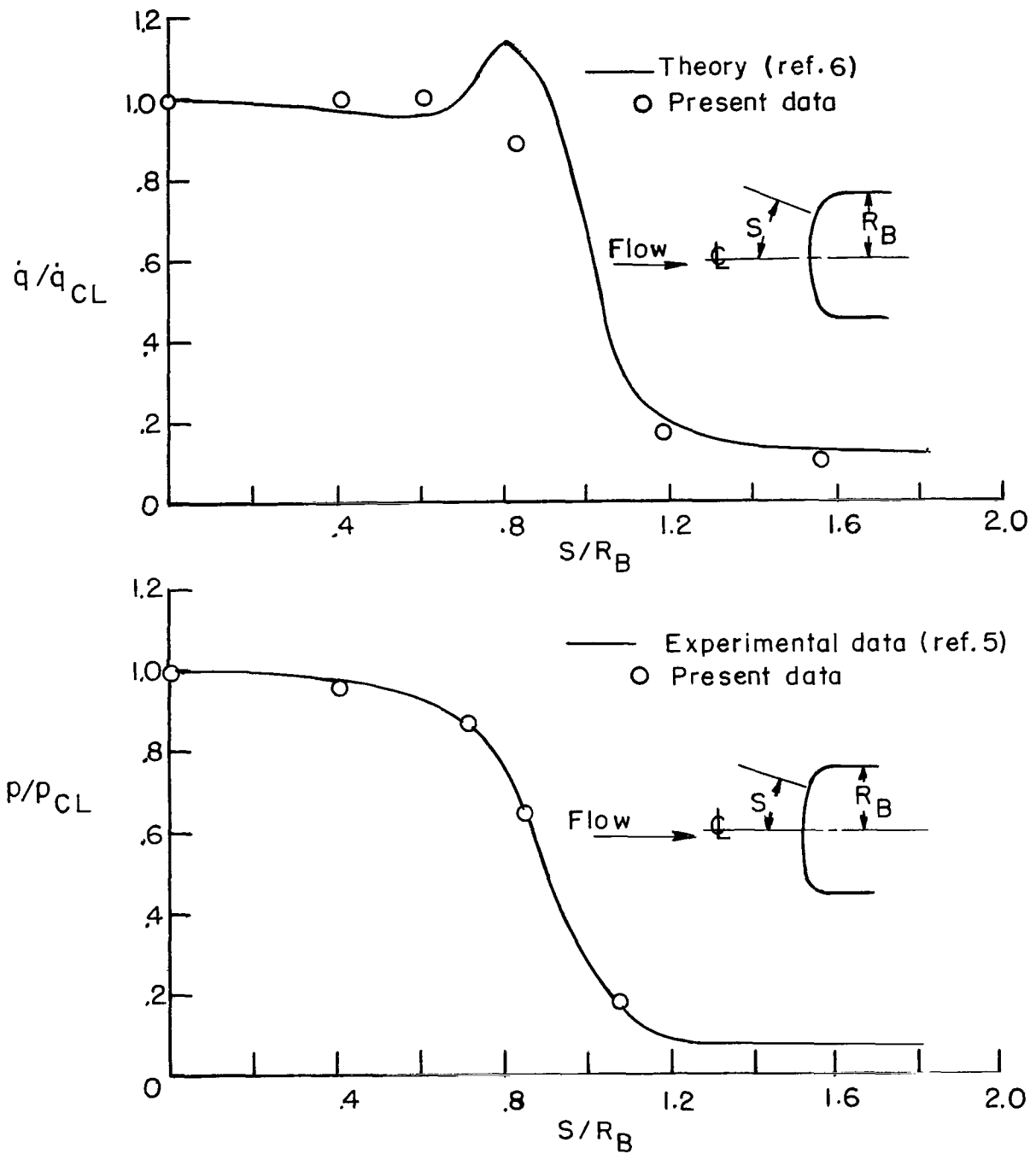
(a) Arc-chamber pressure, 1.2 atm.

Figure 15.- Distribution of heating rate and pressure on probe shape shown in figure 7 or 8. $R_E = 3.82$ inches (9.70 cm) and $x = 0.8R_E$.
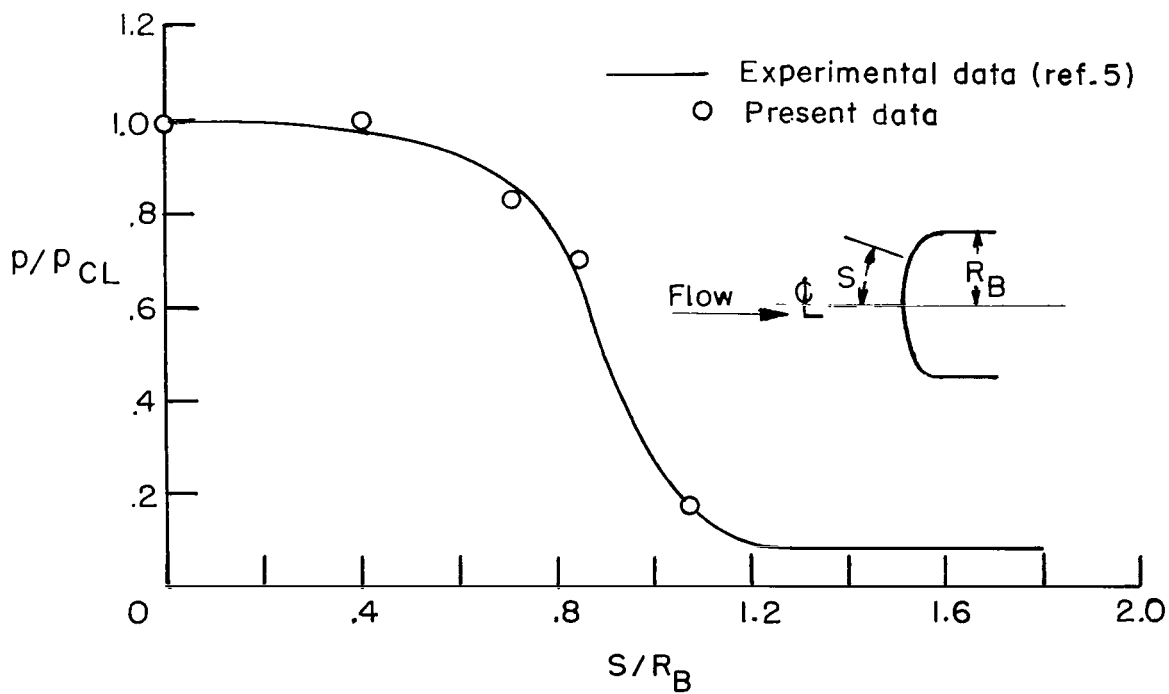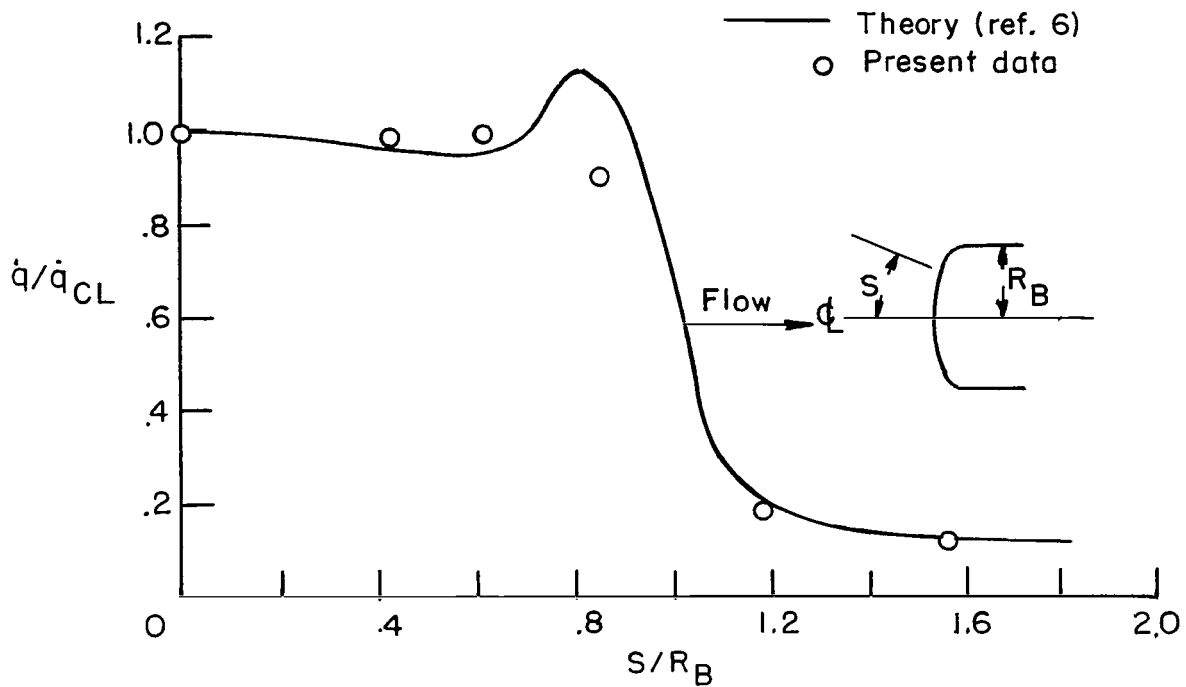
(b) Arc-chamber pressure, 2.0 atm.

Figure 15.- Continued.
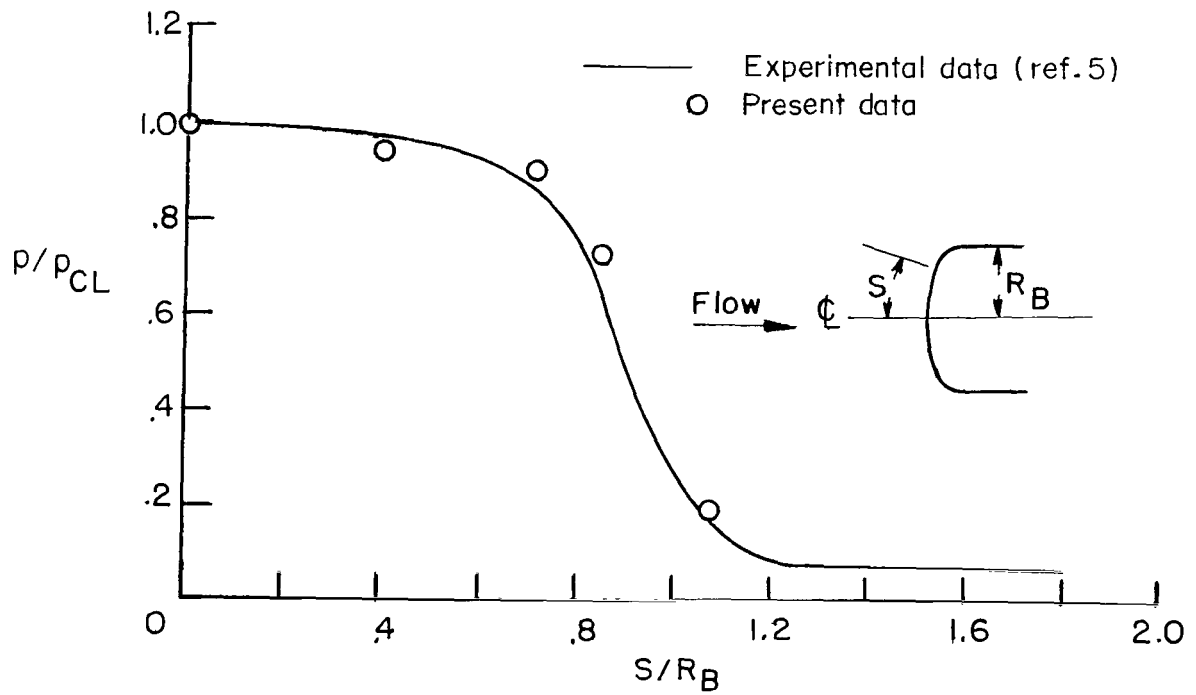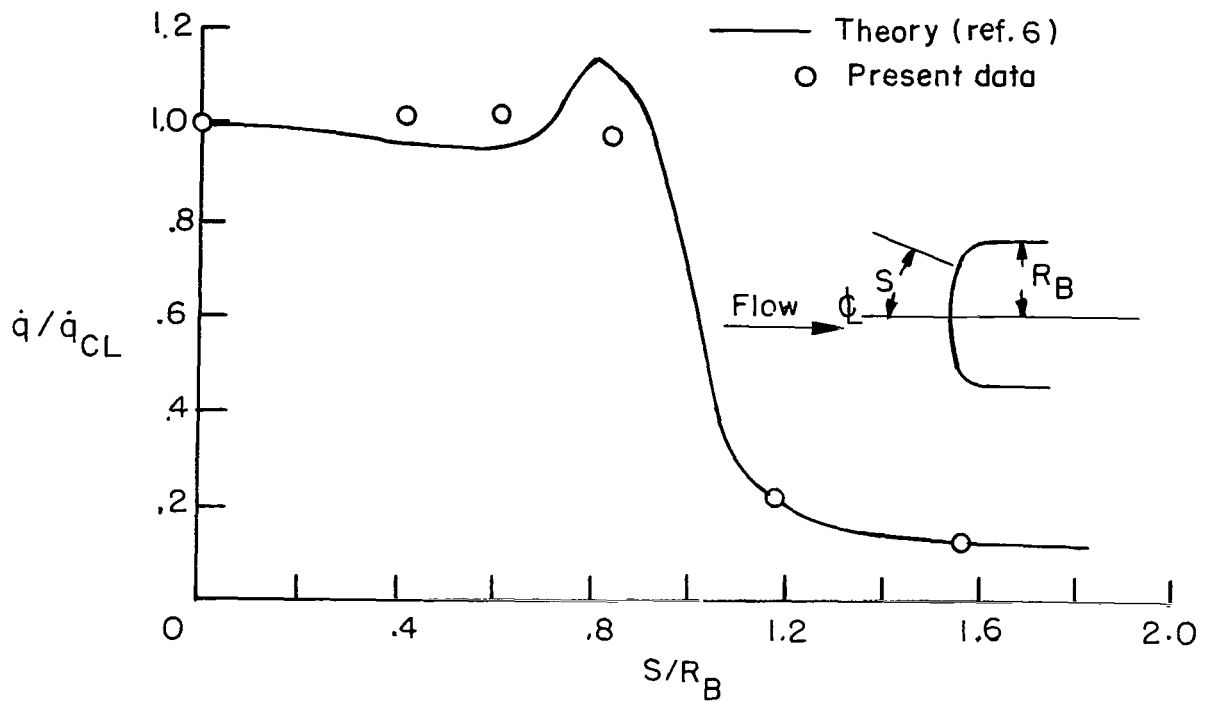
(c) Arc-chamber pressure, 3.3 atm.

Figure 15.- Concluded.
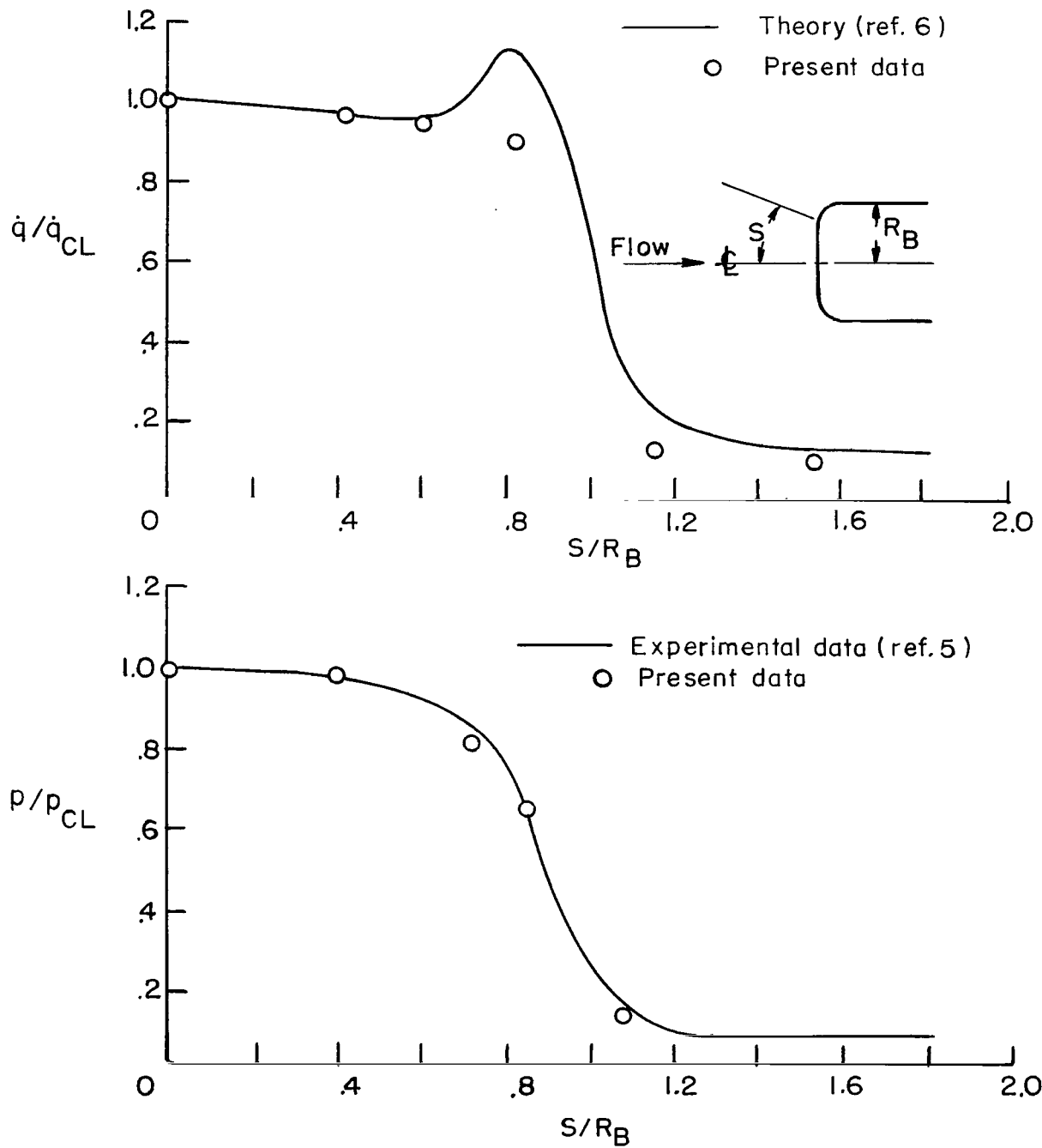
(a) Arc-chamber pressure, 1.2 atm.

Figure 16.- Distribution of heating rate and pressure on probe shape shown in figure 7 or 8. $R_E = 2.30$ inches (5.84 cm) and $x = 0.8R_E$.
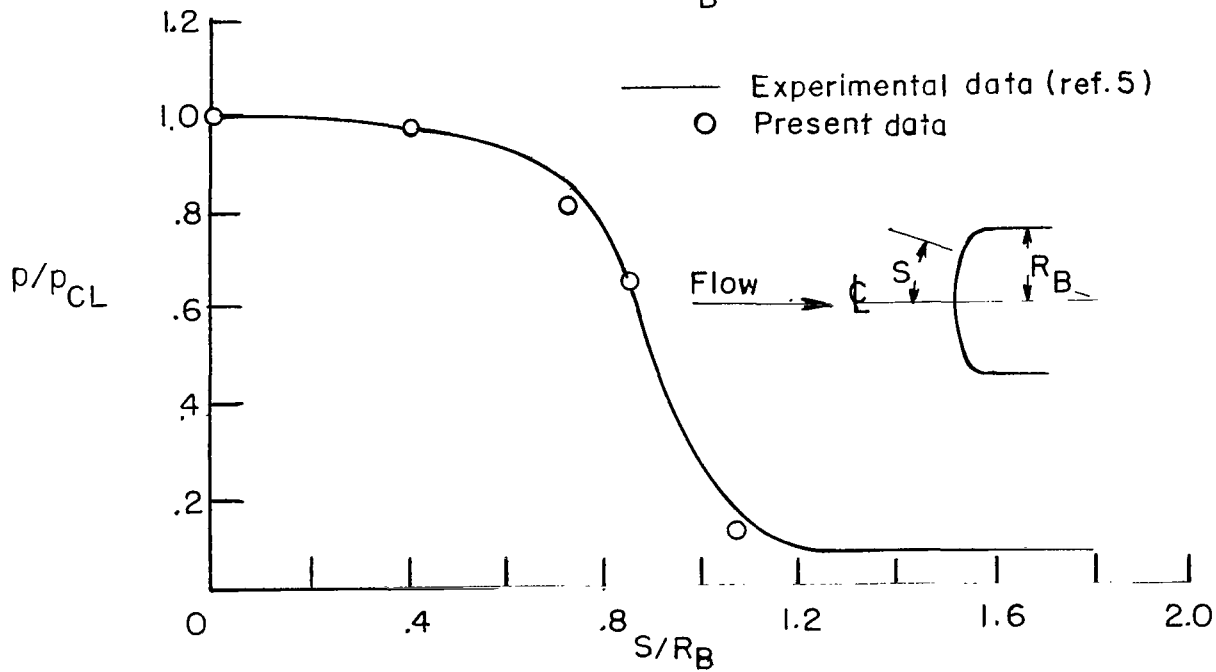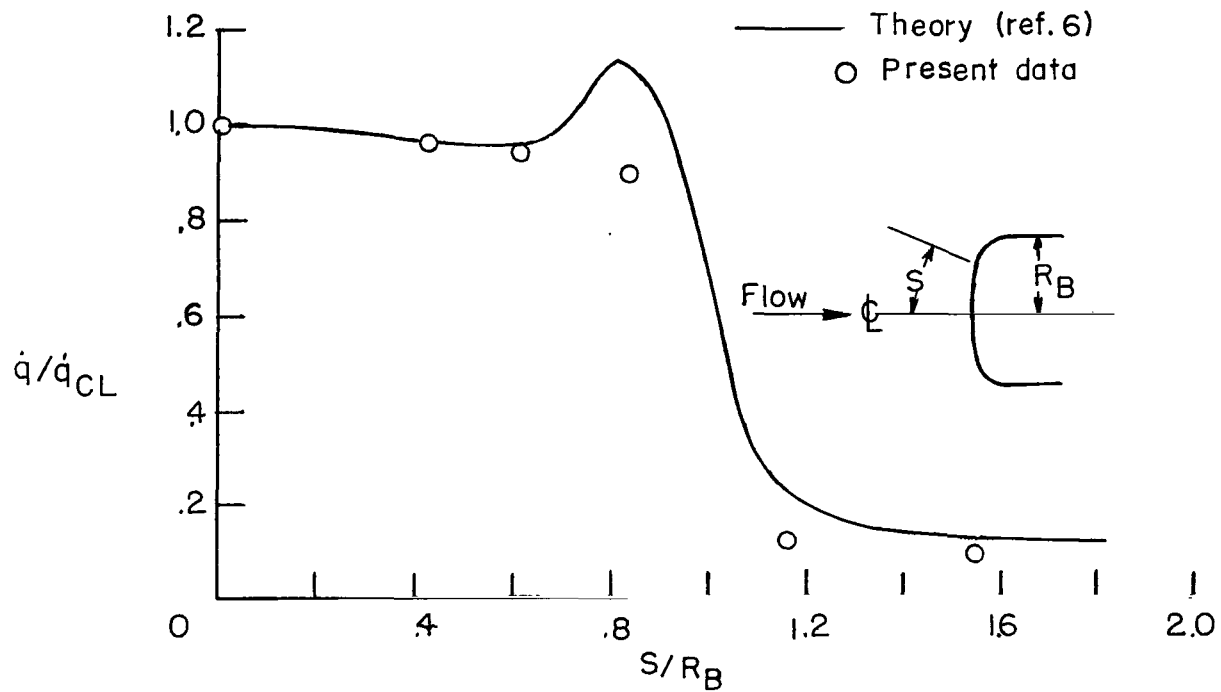
(b) Arc-chamber pressure, 2.0 atm.

Figure 16.- Continued.
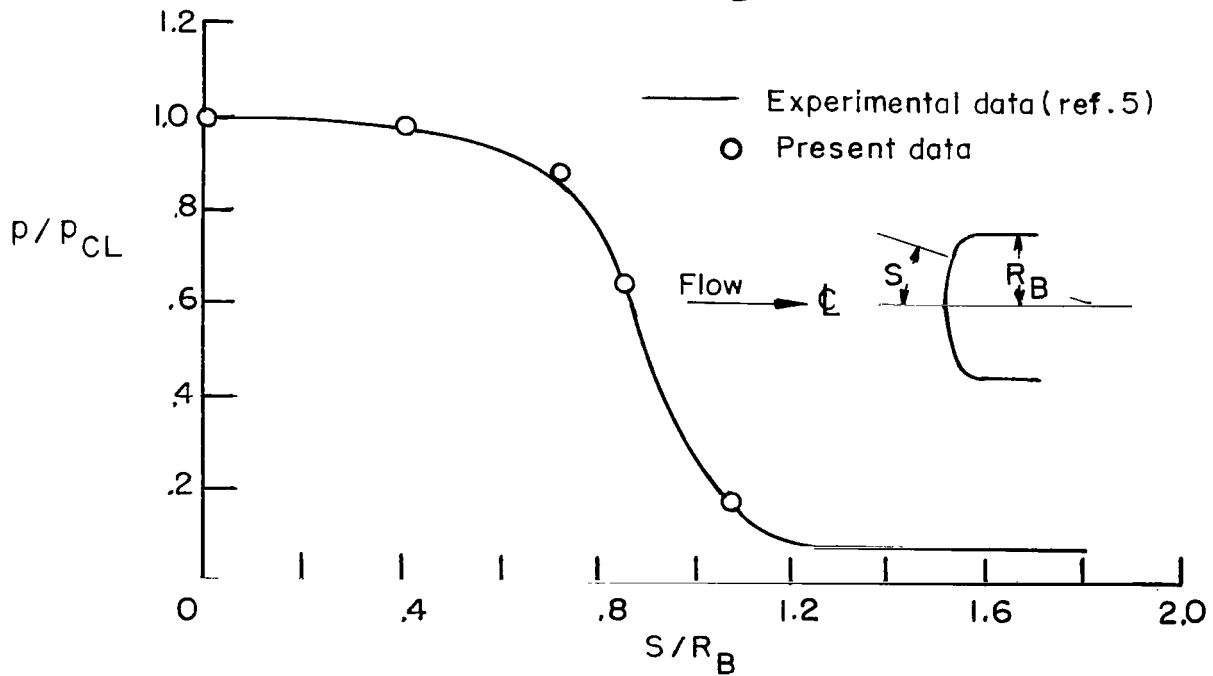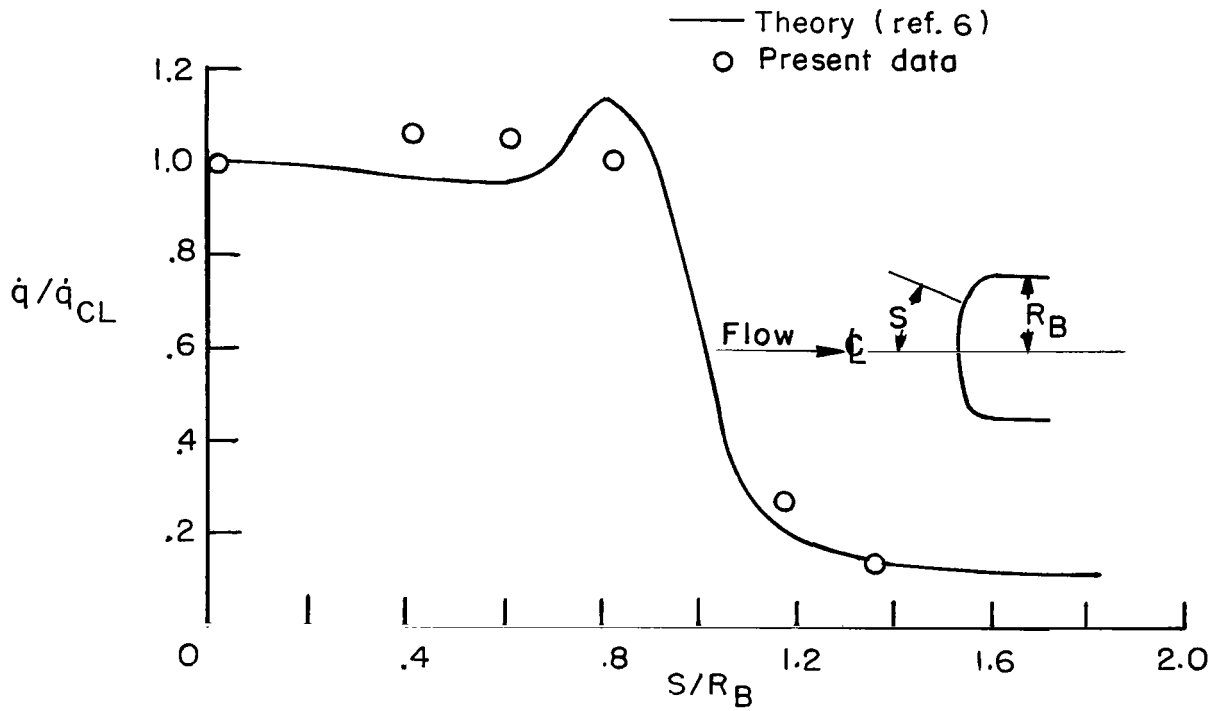
(c) Arc-chamber pressure, 3.3 atm.

Figure 16.- Concluded.
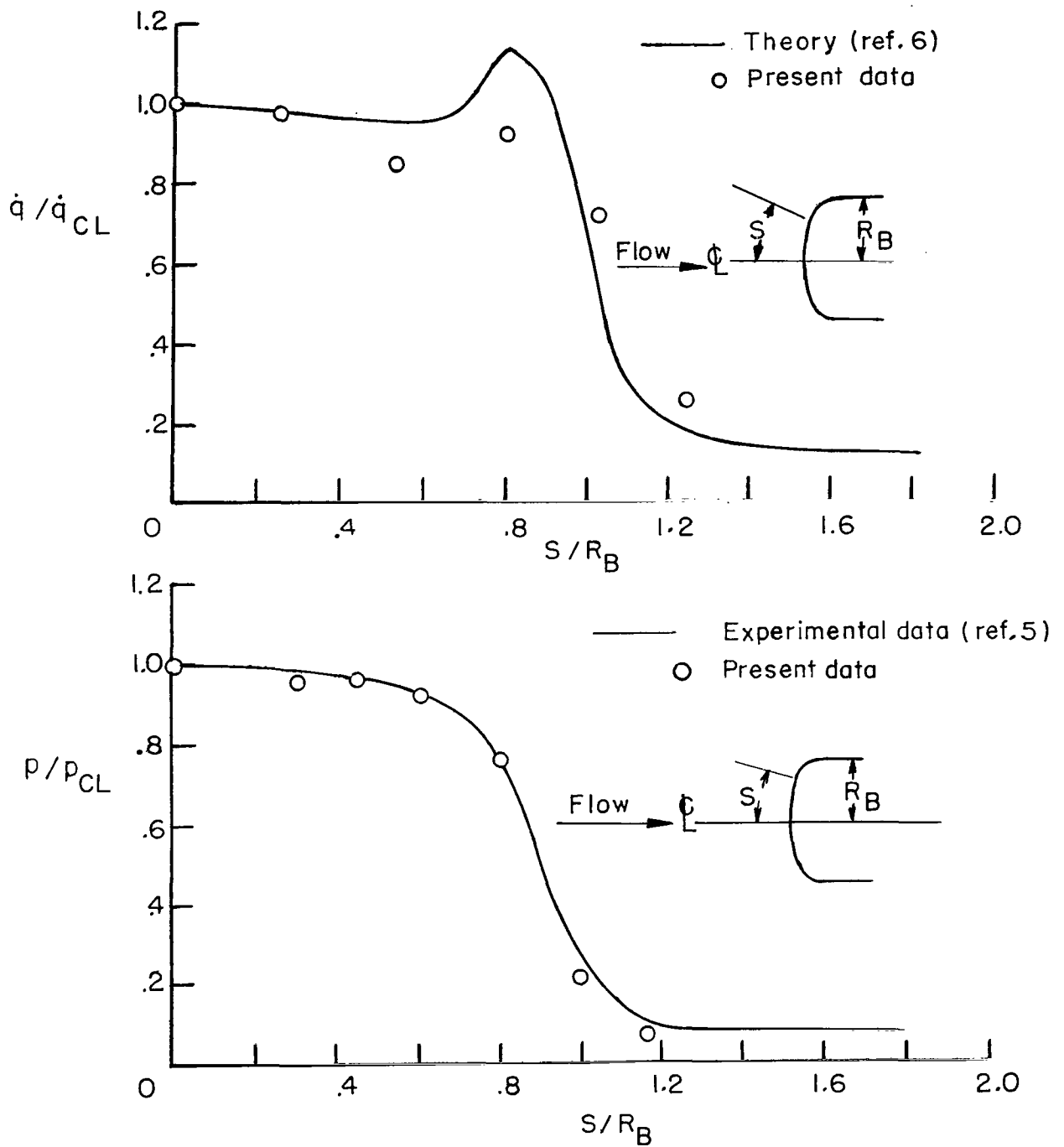
(a) Arc-chamber pressure, 1.2 atm.

Figure 17.- Distribution of heating rate and pressure on probe shape shown in figure 7 or 8. $R_E = 1.00$ inch (2.54 cm) and $x = 0.8R_E$.
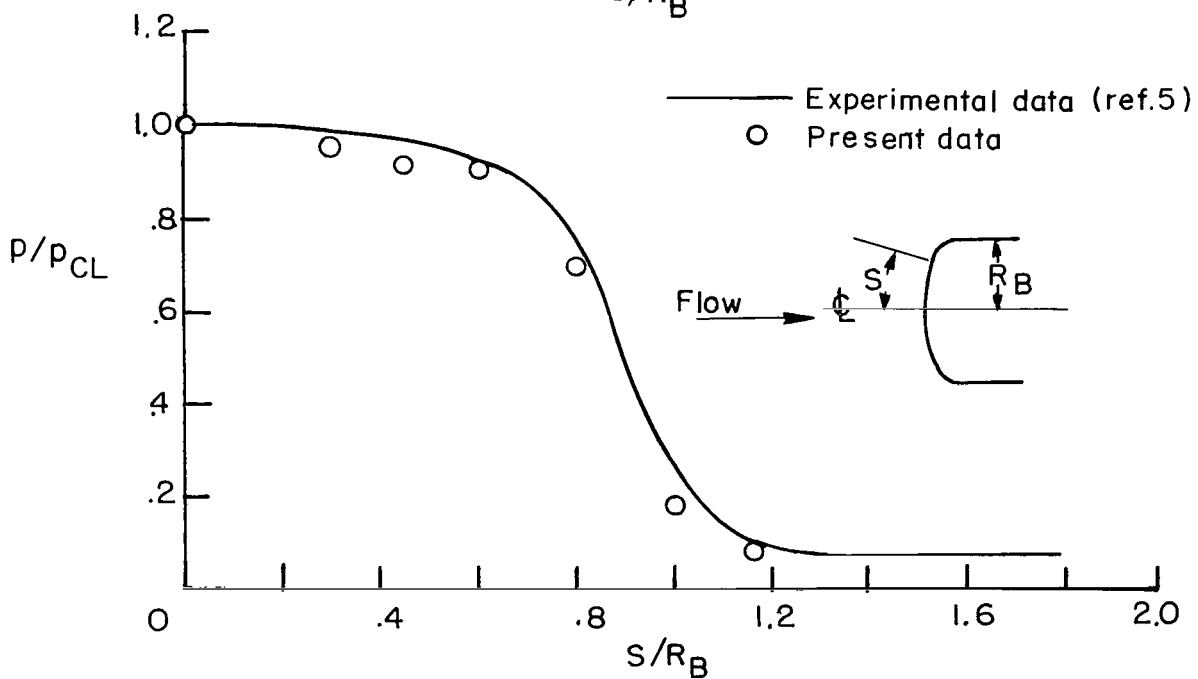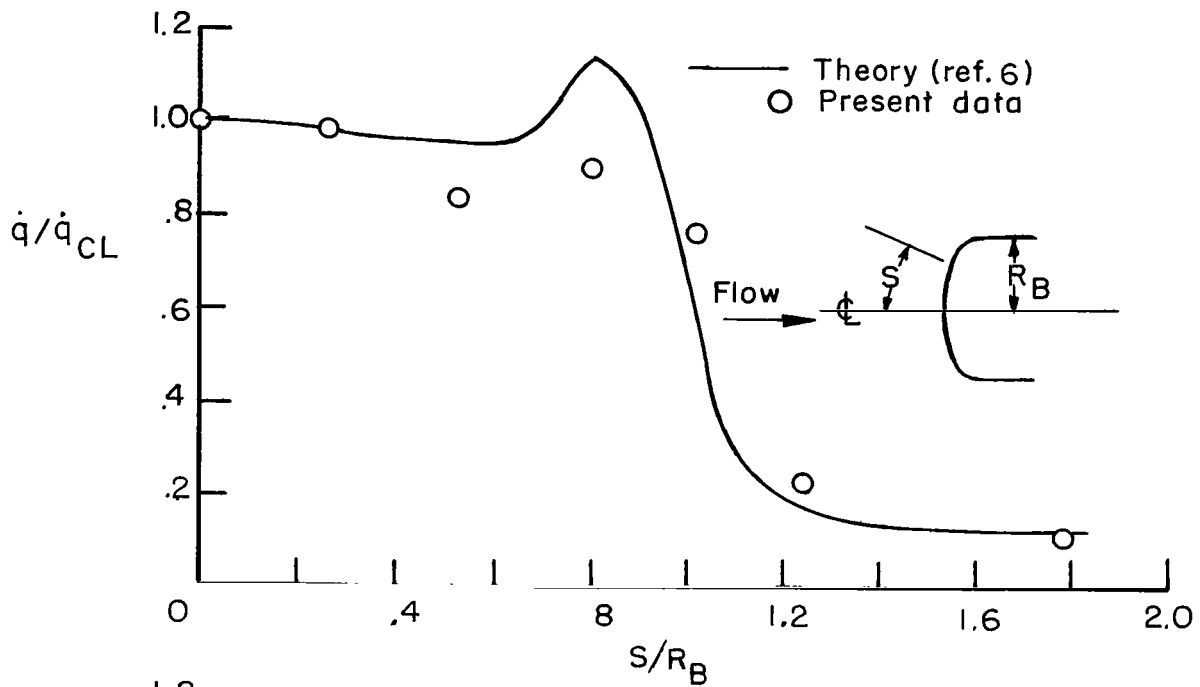
(b) Arc-chamber pressure, 2.0 atm.

Figure 17.- Continued.
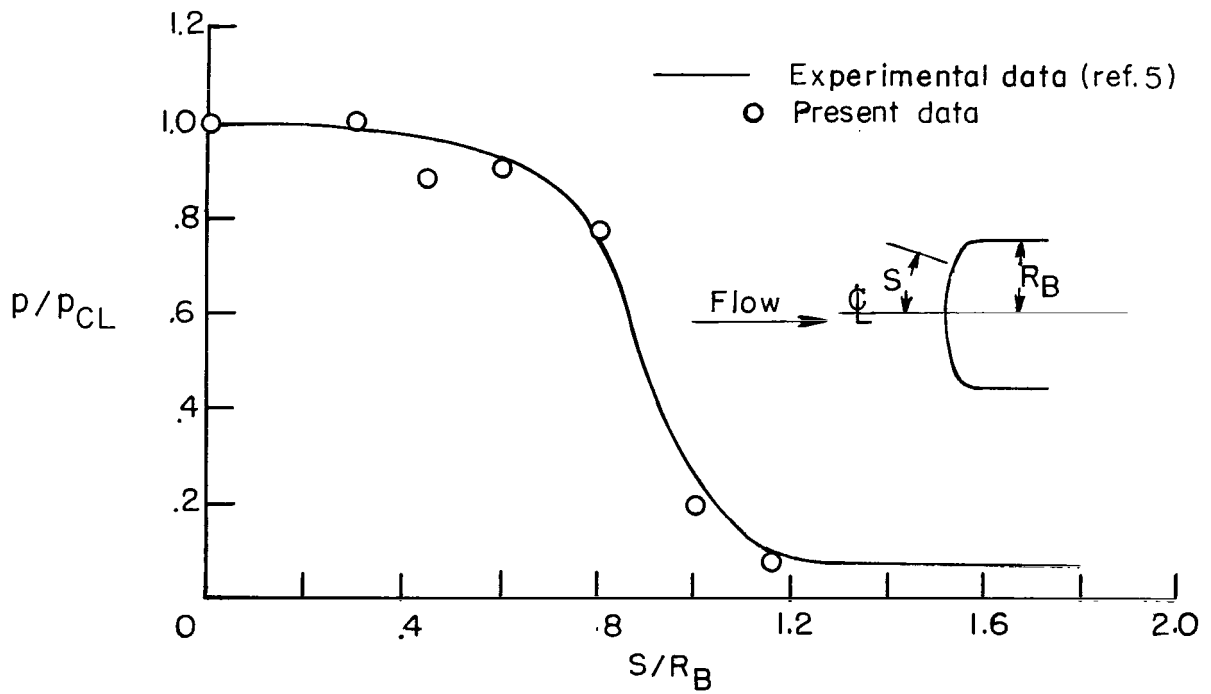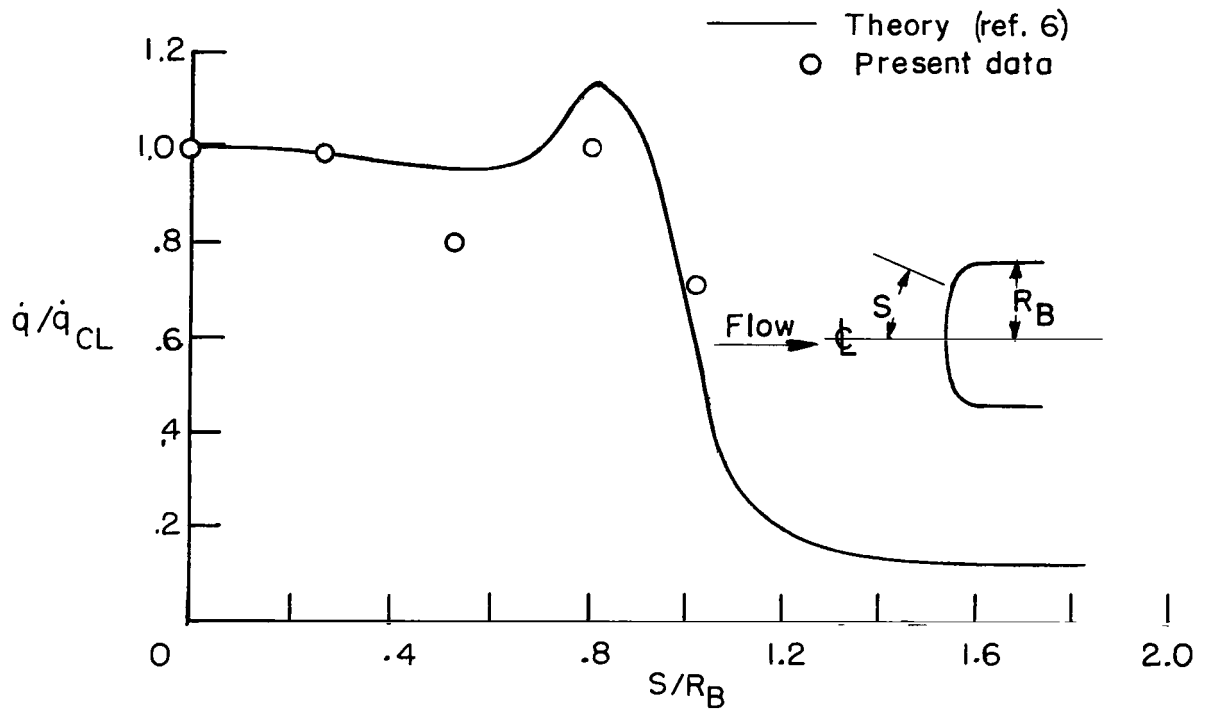
(c) Arc-chamber pressure, 3.3 atm.

Figure 17.- Concluded.
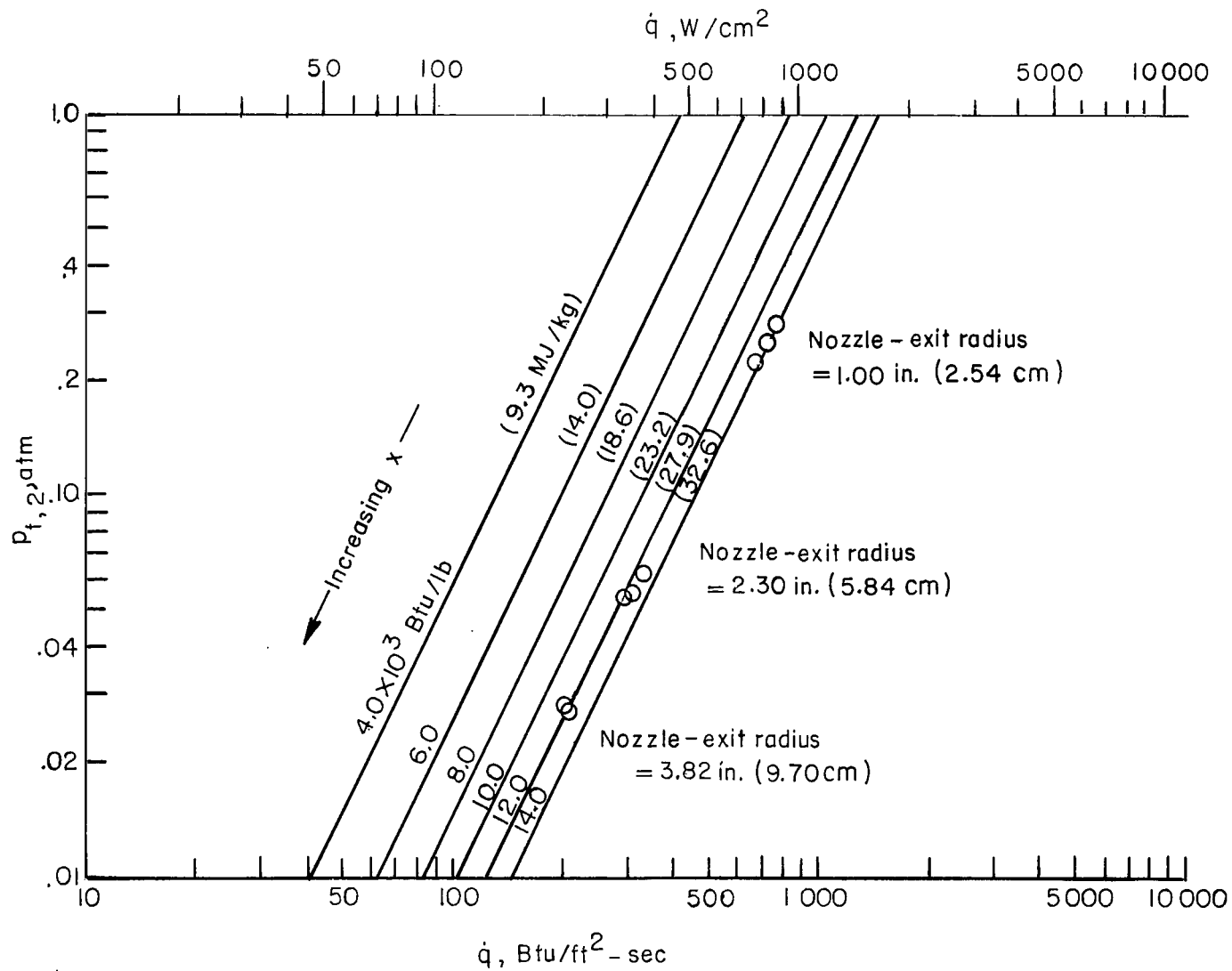
(a) Arc-chamber pressure, 1.2 atm.

Figure 18.- Relationship of heating rate, pressure, and enthalpy at the test-stream center line for all three nozzles. Heating rate is for a 1.0-inch-diameter (2.54-cm) flat-faced probe.
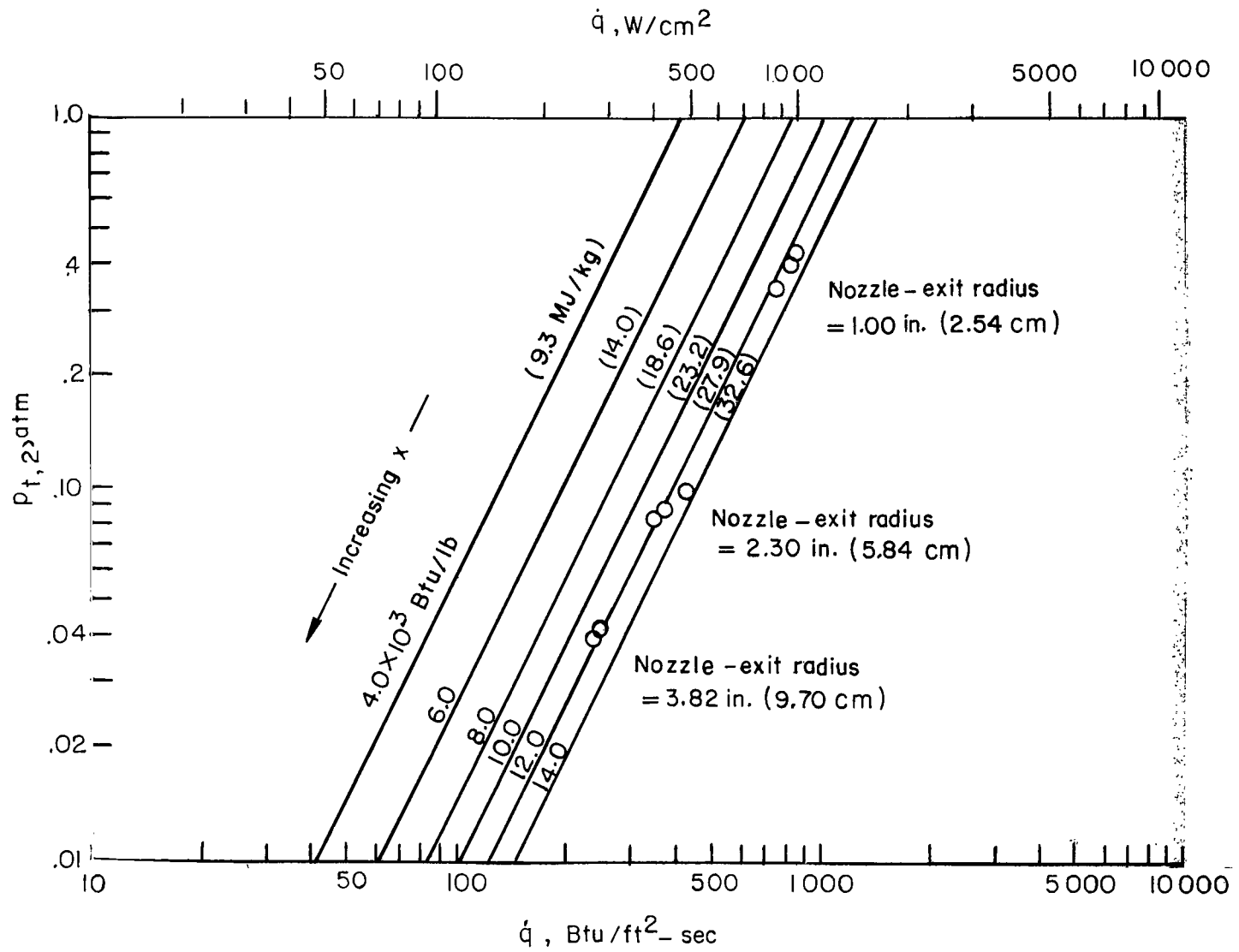
(b) Arc chamber pressure, 2.0 atm.

Figure 18.- Continued.

$\dot{q}$, W / cm^2

Nozzle – exit radius
= 1.00 in. (2.54 cm)

Nozzle – exit radius
= 2.30 in. (5.84 cm)

Nozzle – exit radius
= 3.82 in. (9.70 cm)

$\dot{q}$, Btu / ft^2- sec
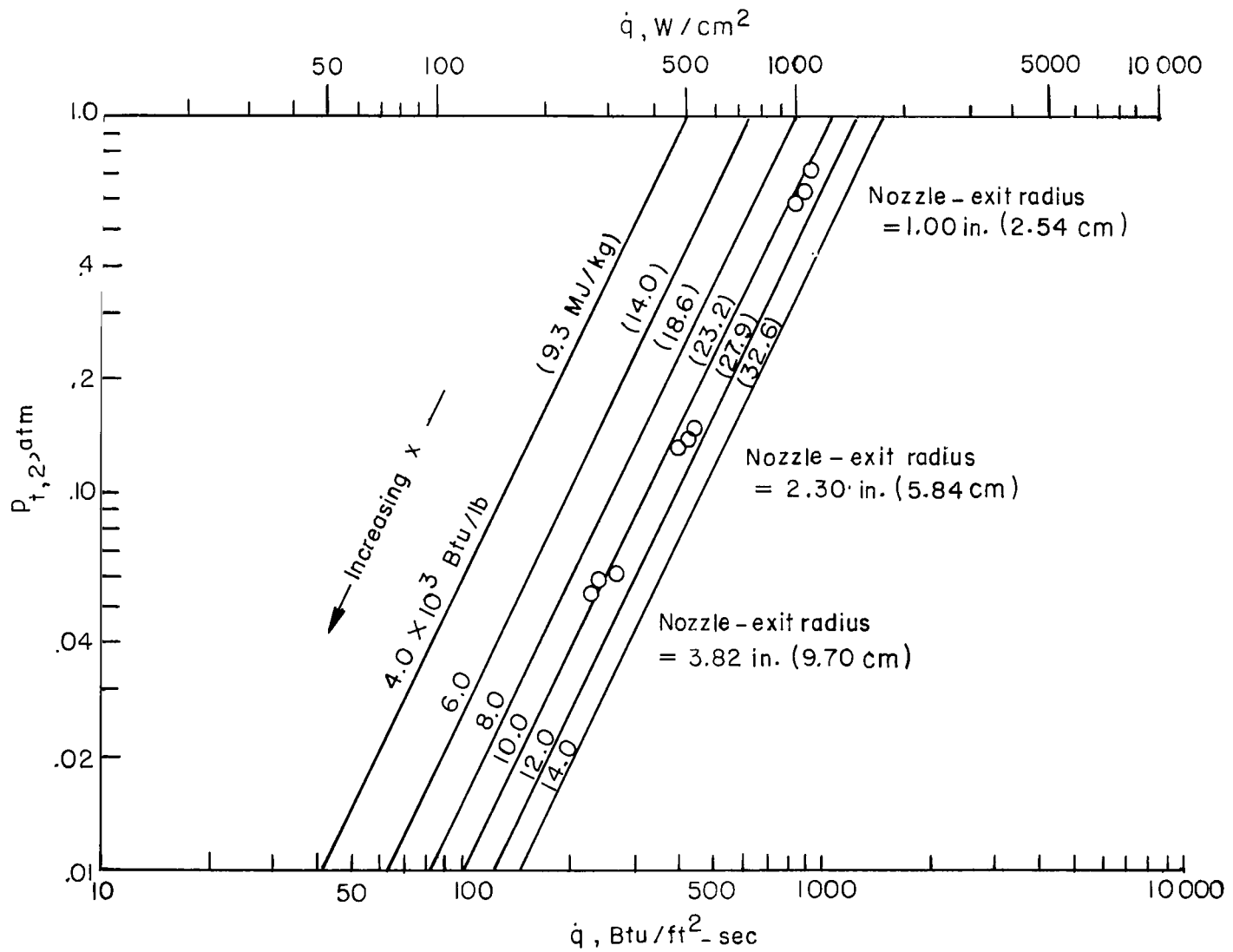
(c) Arc-chamber pressure, 3.3 atm.

Figure 18.- Concluded.

FIRST CLASS MAIL
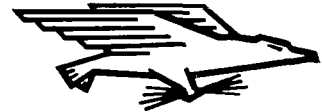
POSTMASTER: If Undeliverable (Section 158 Postal Manual) Do Not Return

·"'The aeronautical and space activities of the United States shall be conducted só as to contribute . . . to the expansion of human knowledge of phenomena in the atmosphere and space. The Administration shall provide for the widest practicable and appropriate dissemination of information concerning its activities and the results thereof."

— NATIONAL AERONAUTICS AND SPACE ACT OF 1958

NASA SCIENTIFIC AND TECHNICAL PUBLICATIONS

TECHNICAL REPORTS: Scientific and technical information considered important, complete, and a lasting contribution to existing knowledge.

TECHNICAL NOTES: Information less broad in scope but nevertheless of importance as a contribution to existing knowledge.

TECHNICAL MEMORANDUMS: Information receiving limited distribution because of preliminary data, security classification, or other reasons.

CONTRACTOR REPORTS: Scientific and technical information generated under a NASA contract or grant and considered an important contribution to existing knowledge.

TECHNICAL TRANSLATIONS: Information published in a foreign language considered to merit NASA distribution in English.

SPECIAL PUBLICATIONS: Information derived from or of value to NASA activities. Publications include conference proceedings, monographs, data compilations, handbooks, sourcebooks, and special bibliographies.

TECHNOLOGY UTILIZATION PUBLICATIONS: Information on technology used by NASA that may be of particular interest in commercial and other non-aerospace applications. Publications include Tech Briefs, Technology Utilization Reports and Notes, and Technology Surveys.

Details on the availability of these publications may be obtained from:

SCIENTIFIC AND TECHNICAL INFORMATION DIVISION

NATIONAL AERONAUTICS AND SPACE ADMINISTRATION
Washington, D.C. 20546